Journal of Dynamic Behavior of Materials (2022) 8:178–213
https://doi.org/10.1007/s40870-022-00331-0

REVIEW ARTICLE

Measuring the Effect of Strain Rate on Deformation and Damage in Fibre-Reinforced Composites: A Review

J. I. Perry[1] · S. M. Walley[1]

Received: 21 June 2021 / Accepted: 21 January 2022 / Published online: 15 February 2022
© The Author(s) 2022

Abstract

This review aims to assess publications relevant to understanding the rate-dependent dynamic behaviour of glass- and carbon-fibre reinforced polymer composites (FRPs). FRPs are complex structures composed of fibres embedded in a polymer matrix, making them highly anisotropic. Their properties depend on their constituent materials as well as micro-, meso- and macro-scale structure. Deformation proceeds via a variety of damage mechanisms which degrade them, and failure can occur by one or more different processes. The damage and failure mechanisms may exhibit complex and unpredictable rate-dependence, with certain phenomena only observable under specific loading conditions or geometries. This review focusses on experimental methods for measuring the rate-dependent deformation of fibre composites: it considers high-stain-rate testing of both specimens of 'simple' geometry as well as more complex loadings such as joints, ballistic impact and underwater blast. The effects of strain rate on damage and energy-based processes are also considered, and several scenarios identified where strength and toughness may substantially decrease with an increase in strain rate.

Introduction

Fibre reinforced plastic (FRP) composites have been made with a wide range of constituent materials, weaves, geometries and fibre fill fractions, and so despite a large amount of published experimental data, true like-for-like comparisons between studies are rarely possible. Most tests have been performed on a specific material of interest to the authors' particular application, and – particularly at high rate – comprehensive understanding of the underlying mechanisms remains limited.

Composites made from long fibres arranged in layers or 'plies' exhibit long-range anisotropy and order. This directionality means damage mechanisms and failure modes will depend on the specific loading conditions and specimen geometry, as well as factors such as rate and temperature dependence. Further, whereas metals can absorb energy via elastic and plastic deformation without significant reduction in strength, the dominant process of energy absorption in composites occurs via damage such as matrix cracks, debonding, delamination and fibre pull-out and/or breakage – all of which may degrade the material to a greater or lesser extent. Each of these has an associated rate-dependence, so in some circumstances a shift in failure mode is observed as strain rate is increased. The overall rate-dependence of an FRP specimen will be controlled by the rate-dependence of each of these competing damage and failure mechanisms, in addition to the properties of the constituent fibres and matrix themselves.

Two recent review articles provided a nucleus for this work. First, Zhang et al. [1] presented a review of the properties of glass fibre reinforced plastics (GFRPs). While their interest was mainly in pultruded fibres, the lack of directly relevant data led them to consider composites fabricated via other techniques in some detail. Second, a review by Kidane et al. [2] of strain rate effects in the shear loading of polymer matrix composites provided understanding of multi-directional behaviour. This is of particular importance for the understanding of the highly directional nature of glass and carbon FRPs. Many of the challenges associated with high strain rate testing of composites have been known for some time, and are eloquently described as follows by Hamouda et al. [3]:

> The characterization of the constituents is indeed important in assessing the performance of composites of the fibre-reinforced type, however, the complex interaction occurring between the reinforcing fibres

✉ J. I. Perry
jip24@cam.ac.uk

[1] Cavendish Laboratory, University of Cambridge, J.J. Thomson Avenue, Cambridge CB3 0HE, UK

and the matrix phase results in difficulties in assessing the rate dependency of the constituent phases. Thus, whilst some progress in extending dynamic test techniques to composites and developing new rate dependent tests for composites has been made, assessing the mechanical behaviour of composites will rest with the ability to clearly distinguish the response mode of the specimens tested, i.e. to specifically note the geometrical and material properties features associated with the specimens tested.

This review aims to draw together experimentally driven research from a wide range of materials and types of experiment to highlight particular physics of interest with regards to high strain rate loading of FRPs. Central to this is the concept that FRPs are structural materials whose properties depend not only on 'intrinsic' material properties but also on meso- and even macro-scale structure. As such, particular attention is paid to evidence of unexpected phenomena which may arise because of these FRP-specific quirks, most notably where high strain rate loading may present comparatively greater risk of damage or failure than under quasi-static conditions. The focus here is primarily on macro-scale deformation and failure properties, with reference made to damage and failure modes within that context. A specific, detailed discussion of the rate dependence of fracture mechanics in FRPs is beyond the scope of this review, as it would itself likely warrant an article of similar length.

It should be noted that authors use different terms to denote specimen orientation. Where laminas lie perpendicular to the loading direction, the terms 'out-of-plane', 'transverse', 'through thickness' or '90°' are common. 'In-plane loading' is usually reserved for woven and [0°,90°] layups, while 'longitudinal' or '0°' directions denote loading in the fibre direction of uniaxial materials. 'Off-axis' tests involve non-orthogonality between fibres and loading direction, and may be 'symmetrical' (e.g. ± 45°). Crack propagation and failure are more consistently labelled as in Fig. 1, with 'mixed mode' (usually I & II) loading also possible.

A range of dynamic testing methods have been employed for the testing of composites, examples of which are given in Table 1. Fibre-reinforced plastics (glass and carbon reinforcements) began to be widely used in the aerospace industry in the 1960s as they are both light and strong (have a high specific strength). The major impact threat comes from so-called 'foreign object damage'. This can be low velocity (someone drops a spanner during maintenance), resulting in so-called HVID (Hardly Visible Impact Damage). Or it can be high velocity (due to stones, nuts and bolts etc. left lying around on the runway and thrown into the air during take-off and landing), resulting in BOID (Bloody Obvious Impact Damage). HVID is more insidious as it can cause catastrophic failure without warning. BOID can be seen by eye and dealt with, though of course failure may occur simultaneously with its formation, so various non-invasive techniques have been developed to detect HVID. Damage studies are performed either by low velocity gas guns or by drop-weight studies using blunt-ended rods or darts.

Table 1 Summary of systems used for dynamic loading. From [3]

Mode	Applicable strain rate (s^{-1})	Testing techniques
Compression	< 0.1	Conventional testing machine
	0.1–100	Servo-hydraulic machine
	0.1–500	Cam plastometer and drop test
	200–10^4	Hopkinson pressure bar
	10^4–10^5	Direct impact using air gun apparatus
Tension	< 0.1	Conventional testing machine
	0.1–100	Servo-hydraulic machine
	100–10^4	Hopkinson pressure bar in tension
	10^4	Expanding ring
	> 10^5	Flyer plate
Shear	< 0.1	Conventional testing machine
	0.1–100	Servo-hydraulic machine
	10–10^3	Torsional impact
	100–10^4	Hopkinson pressure bar is torsion
	10^3–10^4	Double-notch shear and punch
	10^4–10^7	Pressure-shear plate impact

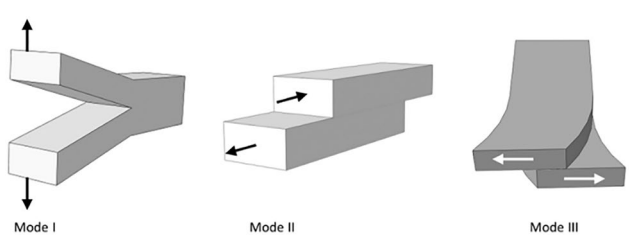

Fig. 1 Schematic diagrams of various types of loading for crack induction. From [4]

First applied to fibre composites in the 1970s, Split Hopkinson Pressure Bar (SHPB) experiments have become arguably the most common means of probing high-strain-rate loading. However, application of SHPB testing to composites is not easy: It requires the coupling of a propagating elastic wave in a cylindrical metal bar into a small specimen of highly anisotropic (but spatially ordered) composite, without introducing significant dispersion, edge effects or stress concentration. End-friction is also a potential concern [5]. As SHPB experiments are designed to measure flow stress, early-time strain data prior to force equilibrium is not reliable or straightforward to analyse [6], and achieving a constant strain rate in SHPB loading [7] is a particular concern

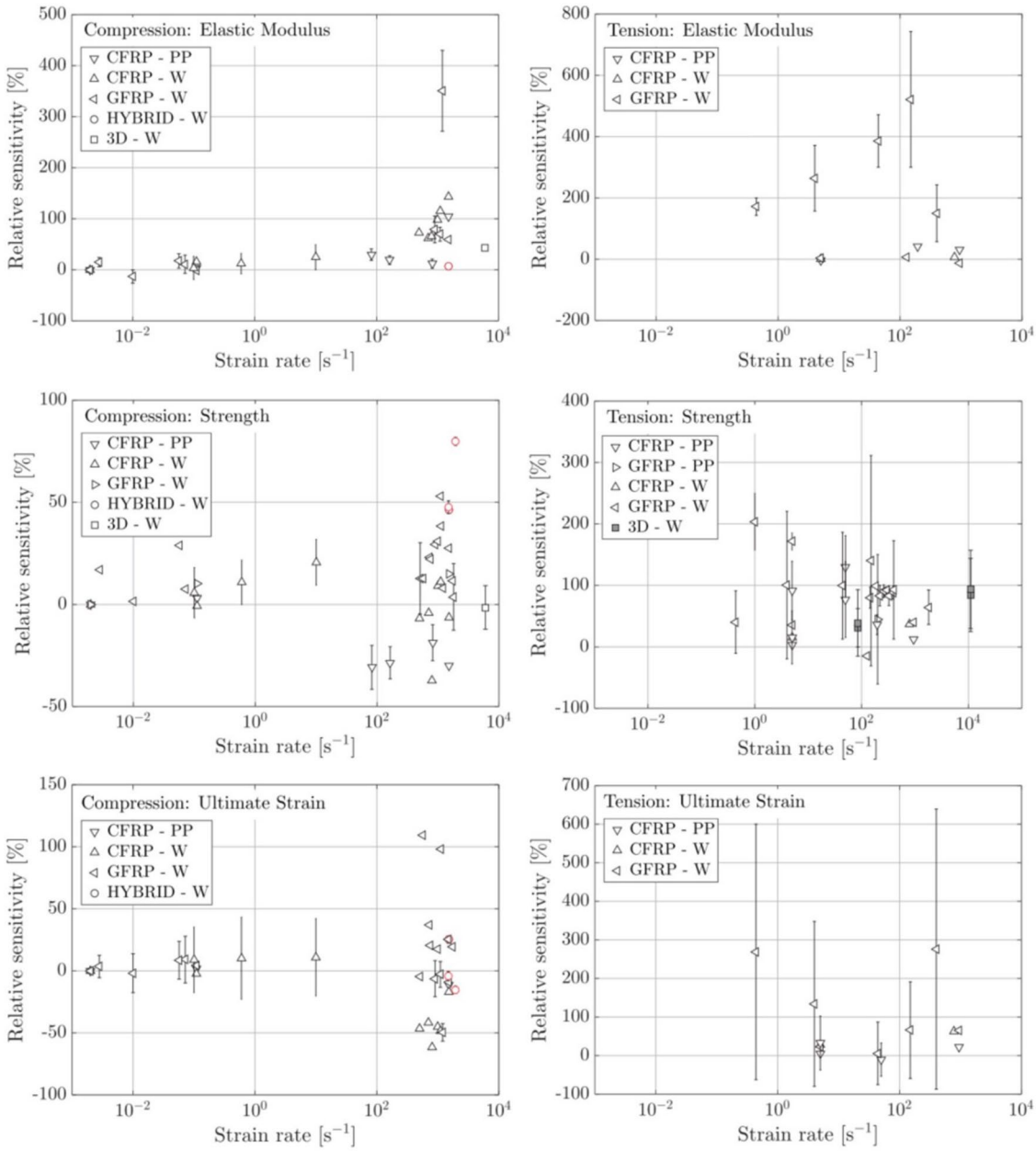

Fig. 2 Strain-rate sensitivity of various composites under interlaminar loading. 'PP' and 'W' denote pre-preg and plain weave reinforcement respectively. The error bars denote the range of reported sensitivity. From [11]

both in long specimens and where failure strains are very small [8]. As a result, low strain mechanical parameters such as dynamic moduli cannot be measured reliably or accurately using the SHPB. Pulse-shaping is sometimes used to keep the strain rate more constant throughout loading [9]. Tuttle & Brinson point out that strain gauges affixed directly to composite samples with epoxy may well fail before the specimen does [10], and the authors offer further commentary on alignment issues, off-axis testing and other concerns.

Van Blitterswyk et al. [11] recently provided a review of interlaminar properties of composites at high strain rates, which highlighted difficulties with the SHPB (and other) experiments. They emphasised the need for full-field data as opposed to information obtained from only a single point on the specimen. Furthermore, they presented a series of charts detailing relative sensitivity to strain rate of key interlaminar properties, which illustrate the lack of agreement between studies as to their strain rate sensitivity (Fig. 2). In recent years full-field measurement techniques have become much more common where non-uniform strains are expected: Digital Image Cross-Correlation (DICC) is the most common approach; more bespoke methods, such as Digital Gradient

Sensing [12] (which can be used to measure out-of-plane deformation), have also been developed.

As inspection of specimens post-experiment is of particular interest for damage-driven deformation in FRPs, some researchers [13–15] have used a 'reaction mass' design of SHPB, whereby the input bar is stopped after a pre-set time in order to avoid repeat loading. Such a setup is challenging to implement well, and reduces the flexibility of the system to tune parameters or test different materials, so is most suited for single-interest laboratories.

A wide variety of other high-strain-rate experimental methods have been employed to investigate the impact properties of FRPs. A technique has been developed which is part ballistic impact, part Hopkinson bar [16], in which a projectile impacts a 'mitigator', fixed to a specimen held between two 'momentum exchange masses'. Accelerometers and streak cameras are used to measure stress and strain. Moulart and co-workers used a mesh grid (as opposed to the more common speckle pattern) with DICC to study notched composite specimens [17, 18]. Various sample-heating methods have been proposed, such as a novel approach which includes cooling both sides of a central furnace [19]. Dropweight-tensile rigs are also in use [20], and many variations of SHPB apparatus have been attempted, including a spherical indenter design [21]. Govender et al. reviewed 'three-point bend' SHPB designs, most of which involve a two-pronged mounting fixture being added to either the input or output side of the specimen being loaded [22].

There have been very few studies of the Taylor impact of rods made from fibre-reinforced composites. The following are the only published papers we know of: [23–26]. Bourne and co-workers machined 7.6 mm diameter Taylor impact cylinders from a multilayer carbon fibre reinforced toughened epoxy [24]. Specimens were machined out of the panel with three different orientations of their axes with respect to the plane of the panel: 0°, 45° and through-thickness. Figure 3 presents some of their results for cylinders where the fibres were aligned with the axis of the specimen cylinder (top) and perpendicular to the cylinder axis (bottom), highlighting very different failure modes in the two cases. They discussed the high-speed photographic observations in terms of the known response of fibre-reinforced composites to shock- and elastic-wave loading, but made no comparison with constitutive models for composites, which are still under development [27].

As composites contain many fibres, and thus many fibre-matrix interfaces, analysing the most basic representative system possible can provide insights. Applying a high strain rate tensile load to a single fibre [28] is arguably the simplest such approach, and novel diagnostic options include imaging of a SHPB-driven experiment using a synchroton's x-ray beamline [29]. Chu et al. designed a pull-apart test for a similar glass/epoxy specimen, showing that the debonding force increased by 81% from quasistatic to high strain rate loading, while the crack velocity increased by 16% [30]. There are also many examples of quasistatic fibre-matrix interface experiments, such as Favre & Merienne's pull-out assessment of fibre coatings [31].

Several low-rate experimental methods are also worth mentioning. Mandell et al.'s quasistatic debonding test which probes the response to specific geometries by means of different impactor shapes may offer inspiration for high-rate experimental design [32]. Fibre pull-out [31, 33] and fatigue debonding [34] experiments are common, and the study of interfacial physics and chemistry is much more developed under quasistatic loading conditions [35]. Similarly, beyond the scope of this review is a large body of partially relevant research, from developing and analysing new (e.g. high glass transition temperature, T_g) epoxies [36, 37] to testing of aged composites, sometimes using accelerated aging techniques [38].

Constructing models able to account for the many different types of possible deformation, damage and failure modes is a real challenge, and many models are designed only to replicate a subset of composite behaviour relevant to particular applications. Matrix properties are usually considered to be viscoelastic, viscoplastic or visco-elasto-plastic, while the fibres themselves are invariably elastic. The extreme anisotropy means isotropic approaches are rarely sensible; orthotropic models should account for both longitudinal and shear response to, for example, predict the interlaminar shear failure under oblique compressive loading. Rate dependence is then added as an additional layer of complexity, usually by tuning the relevant parameters based on experimental observations – though other factors such as adiabatic heating may also need to be included. The rate dependence of failure modes, damage localisation and other less easily characterised phenomena are the most significant challenge to include.

Thiruppukuzhi & Sun's attempt to construct a rate-dependent model in stages from constitutive behaviour, consideration of individual laminates, and rate-sensitive failure modes is insightful, and outlines a general approach now considered standard [39]. Mariani's delamination model used an energy-based approach, focussing on a particular impact loading failure mode [40]. Karkkainen et al. took a more holistic approach by modelling an unusual SHPB geometry and including rate-dependent and mode-dependent cohesive interface failure [41]. Shokrieh et al.'s approach involved modelling the fibres and matrix separately (in a rate-sensitive manner), then building a micromechanical framework to bring the components together [42]. Recently, molecular dynamics methods have been applied to study the rate-dependence of fibre-matrix interfaces providing

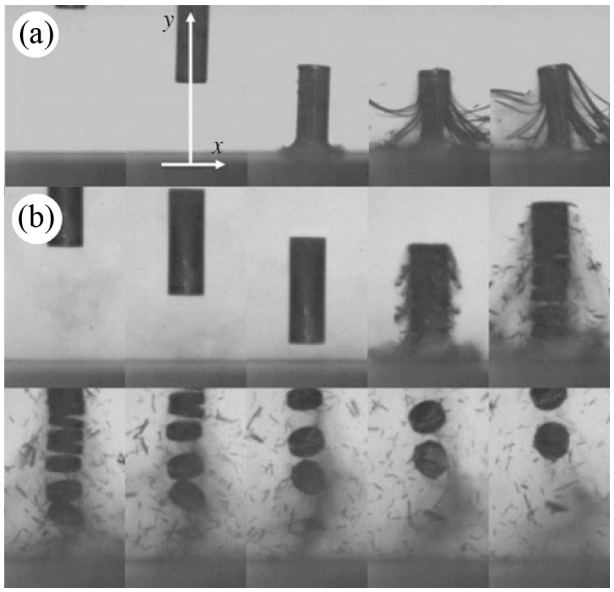

Fig. 3 Selected frames from high-speed photographic sequences of the impact of fibre-reinforced epoxy cylindrical rods. **a** Fibres aligned with the axis of the cylinder. Impact velocity 148 m/s. Interframe time 125 µs. **b** Fibres aligned perpendicular to the axis of the cylinder. Impact velocity 246 m/s. Interframe time 42 µs. From [24]

interesting insights [43]. Analysis shows that the fracture energies should increase with rate as the atoms are less relaxed, and that interfacial failure should become more common at high loading rates due to differences in the strain rate dependency of fibre and matrix.

FRPs are anisotropic composites which deform and degrade via a variety of distinct damage mechanisms; they are arguably 'structures' rather than 'materials'. As such, it is important to consider how high-rate-experiments, many of which are usually applied to isotropic metals and polymers, can be sensibly used to probe the properties of FRPs. The dynamic behaviour of FRPs depends on variables such as specimen and loading geometry, and so it is important to understand published data – and comparisons between studies – in the context of the specific experimental methods employed in each case. In this review, we first consider the most basic tensile and compression loading geometries, followed by a section on off-axis and shear loading (where failure is often induced along weaker inter and intra-laminar failure planes). More geometrically complex scenarios such as ballistic, blast and underwater loading are then considered, as are joints (which are often the weakest parts of FRP structures). Because deformation occurs via damage – a process controlled by energy and work as much as stress and strain – in the third part of the report we consider energy and toughness, repeat loading and geometric effects in some detail.

Tensile Loading

Tensile loading provides the most obviously quasi-one-dimensional configuration, in contrast with compression testing where any failure must involve some lateral motion. However, failure under tensile conditions is often far from one-dimensional, depending on the fibre layup relative to the loading direction. This section focusses on the effects of strain rate on parameters such as failure stress, strain and modulus. Damage and failure mechanisms also show some rate dependence, and these are discussed in more detail later. A wide variety of tensile testing geometries have been used in composite testing, some of which are shown in Fig. 4.

Early dynamic experimental methods were developed from quasistatic equivalents, and their findings were primarily qualitative and comparative rather than quantitative. For example, Almahdy & Verleysen discuss some of the challenges of high strain rate tensile testing, notably explaining that 'classical' SHPB analysis is insufficient due to the deformation being non-uniform [44]. Because of the non-uniformity, strain gauges glued to the surface of the central section of a specimen [45] have largely been superseded by full-field diagnostics such as DICC [46]. Indeed, some novel attempts at measuring full-field displacement pre-date modern computational methods: Armenàkas & Sciammarella, for example, applied photosensitive emulsion to a specimen surface and then optically projected a fine grating onto the emulsion so as to create a grid pattern photographically. The dynamic deformation was then recorded using a high-speed rotating mirror camera [47]. In this quite remarkable paper, significant anisotropy in strain across the material was observed.

Because composites can be very strong in the direction of fibres (particularly unidirectional materials), care must be taken when considering how to grip each end of the specimen to hold it without causing damage. To give a few examples from lower rate experiments, 'double tabs' bonded to both ends to better distribute the gripping stress have been recommended [49]. Use of a single material cut with much wider end-tabs [50], gluing steel tabs to each end of a composite specimen [45], and a combination of narrower neck region and punched holes in each end section (rather than relying on gripping alone) [51] have all been attempted.

An early example of the importance of careful grip design at high rate comes from Ross et al. [52], who in comparing threaded and dumbbell specimens found that data obtained using dumbbell specimens contained a 'wobble' or dip during initial loading as the specimen slipped in its grip. The 'modern' tensile SHPB arrangement was likely first deployed to test composites in the 1990s. In that decade, one early study was of glass/epoxy composites, using epoxy to fix a specimen with a central section waisted in

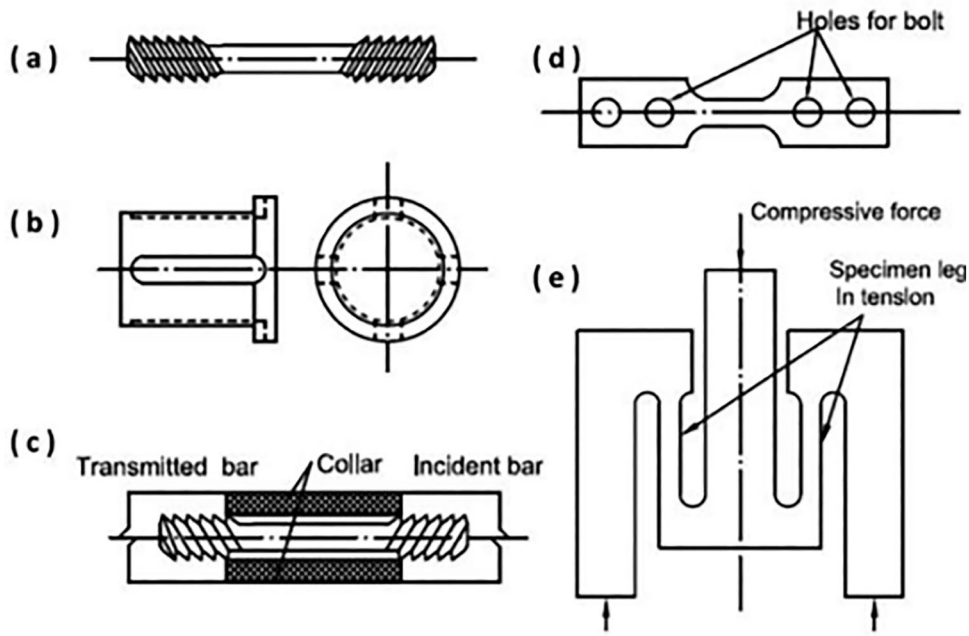

Fig. 4 Different specimen configurations used for high strain rate tensile testing: **a** end-threaded cylinder, **b** 'hat' specimen, **c** end-threaded specimen with collar, **d** tensile specimen with bolt grips, **e** 'M-shaped' specimen. From [48]

both perpendicular directions [53]. Their specimen was 'unidirectionally arranged' in the test section, while 'orthogonally arranged' at both ends. The three most commonly used gripping methods for tensile samples are: (a) adhesive (usually laterally across long end-grips to increase the area of contact); (b) wedge, T-shape or dumbbell obstructive grips; and (c) lateral compressive grips.

In some cases, grips may fail at the end tabs for 0° testing [54]; specimens with multiple fibre orientations are generally weaker; one epoxy-fixed specimen of [0/45/90/-45] graphite/epoxy failed in the central section at ca. 500 MPa [55]. Mechanical clamping by means of bas-relief and bolting has also been attempted, but concerns regarding slipping and noisy data led the authors to instead attach their specimens to the steel fixtures with epoxy (Fig. 5) [56]. Given the strongly anisotropic nature of composites, different specimen geometries for fibre-direction and transverse samples may be preferable [57]: For through-thickness samples, a short, waisted disk glued to the flat ends of the sample holders was used – the short sample accounting for the low sound speed in that direction. This meant there was no need for high-strength grips (Fig. 6 top). Along the fibre direction, a wedge-shaped sample was held in place within a slotted mount (Fig. 6 bottom). In a rare example of such high failure stresses being achievable in a high strain rate experiment on FRP, in order to successfully grip s-glass/epoxy composites Gerlach et al. [58] chose adhesive bonding over bolted or screwed joints, but added a 'lightweight inertial gripping mechanism', which allowed loading of the specimens to the point of fibre failure at ca. 3500 N (Fig. 7).

With regards to materials data obtained from tensile SHPB testing, as published studies involve tests on different

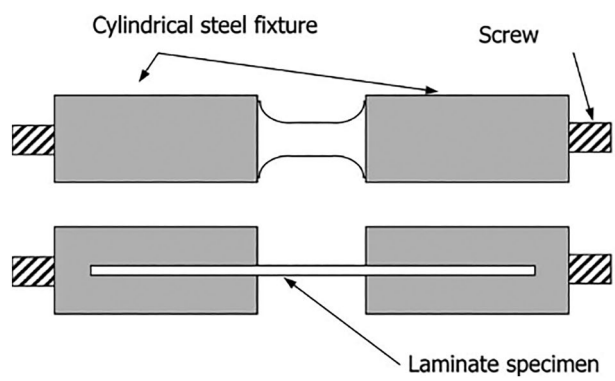

Fig. 5 Design using epoxy to affix the specimens to the steel fixtures. From [56]

materials, with various types of fibre, matrix materials, layups and loading methods, it is perhaps unsurprising that the results are not always consistent. However, the literature contains a large amount of useful information which is summarised below.

In 1983 Harding and Welsh [59] described a tensile SHPB experiment utilising a hollow 'weigh bar' tube containing both the specimen and inertia bar, where a flat specimen (similar to those used in low rate experiments) was attached to the bars with epoxy and loaded in tension. No discernible rate dependence in strength was observed for CFRP, while the GFRP samples became notably stiffer and stronger at higher rates. Additionally, the area of damage increased from bring localised around the failure point under quasistatic load, to across the whole specimen at high rate – an observation since corroborated [46, 60, 61]. The same

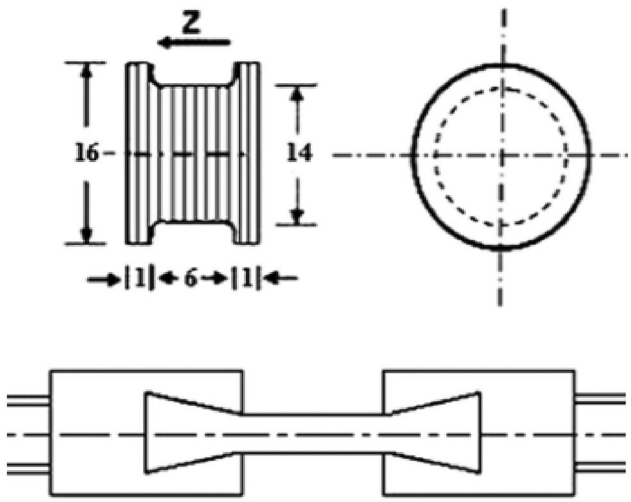

Fig. 6 Different specimen designs employed by the same authors, dependant on orientation of the fibres. Top: through-thickness tests employ a short sample glued to flat mount ends; Bottom: fibre-direction samples wedged into holders. From [57]

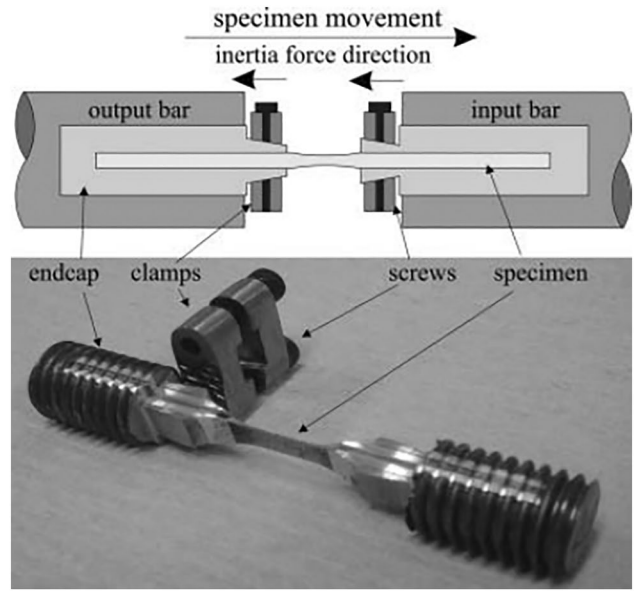

Fig. 7 Top: illustration of fibre failure vs. failure due to pull out (quasi-static data); Bottom: metal clamps used for high-rate tests benefiting from inertia effects. From [58]

authors [62] presented an SHPB analysis of woven composites under tension two years later, studying carbon, Kevlar and glass fibre. Employing a very similar specimen design to before, the aim of their paper was to understand rate dependent behaviour. They argued that the rate dependence of tensile modulus 'derives from the elastic interaction between the reinforcement and the resin matrix, and is determined by the rate-dependence of the matrix strength'. They note that at low rates, fibre pull-out controls fracture strength, while debonding between fractured fibre tows and the resin matrix is more prevalent at higher rates meaning that the matrix itself is actually carrying a significant fraction of the load.

For GFRP in the fibre direction, failure strength certainly appears to increase under more rapid loading. There is some agreement that at high rates the modulus increases with strain rate [50, 53, 58, 61, 63, 64] – though some authors suggest otherwise [65], and one author observed a decrease for moderate rates under tensile loading [60]. Failure strain may increase [58] (particularly in the fibre direction [60]), be uncorrelated [53] or even reduce (for carbon/glass hybrid composites [51]). Properties are fibre-dominated in the 0° direction. Studies on bundles of unbonded glass fibres show that their tensile strength increases with rate [66, 67]. This effect is less pronounced for carbon fibres [68]. In other directions, where failure can occur by tensile or shear failure without breaking any fibres, strengths are significantly lower, and failure is dominated by the properties of the matrix. Higher moduli and failure stresses have been observed at higher strain rates for transverse loading [58, 63, 65].

There are other complications. The strength and failure modes may depend on the quality of manufacturing [58, 63]. The data often exhibits more scatter in high-rate experiments [46, 60], though it is difficult to separate experimental artefacts from random variation in true material response – an issue discussed in more detail later in this review.. Further, the stacking sequence and reinforcement texture may affect the results [69]. Several models have focussed on high strain rate tensile failure [48, 70]. The (relatively) one-dimensional failure modes allow the complexities seen elsewhere to be ignored.

For carbon fibre composites (CFRPs), one study found the stress and strain both increased slightly with rate for 0° loading [71], but only the strain increased with rate in the through thickness direction. Another measured an increase in stiffness for all geometries, with the most notable strength increase with rate observed for ± 45° specimens [72], while a third found little rate (or temperature) dependence in the 0° direction, but a significant increase in strength for 90° at high rate (and low temperature) [56]. Taniguchi et al. used tapered thread and compression ring grips (similar to a collet), and found little rate dependence in the 0° direction, while the transverse (90°) loading was marginally stiffer and ± 45° specimens were significantly stiffer at high rate, though with lower failure strain [73, 74]. Most authors seem to agree that while the carbon fibres themselves do not exhibit rate dependent behaviour, the viscoelastic matrix certainly does, and so composites loaded in tension are more strongly rate-dependent in matrix-dominated directions, with an increase in stiffness (usually) and modulus (sometimes) observed.

Okuyama et al. applied a tensile load to a CFRP specimen with a hole in the middle, and observed the spatial

distribution of strain using DICC and a Shimadzu high-speed camera, [75]. Perpendicular to the loading direction, they found that the strain diminished at a shorter distance from the hole in low rate than in high rate tests, but the opposite was true along the loading direction, so that the strain distribution was laterally narrow and vertically broad at high compared with low rates. The authors suggest a combination of increased stiffness and a change in crack formation may contribute to the changes observed.

Compressive Loading

Dynamic compressive testing of fibre-reinforced polymers does not require end grips, and simpler cylindrical or cuboidal specimens are commonly used. Experiments are more straightforward to perform, and the equipment required is more widely available. Accordingly, the published literature is more extensive. However, many of the other complexities associated with the dynamic behaviour of composites still apply, and damage and failure mechanisms under compression are often more complex than under tension due to the possibility of buckling/kinking of fibres which strongly couples compressive loading to delamination and shear behaviour. Critically, it seems likely that specimen geometry may control the likelihood of other deformation mechanisms such as bending or buckling. In this section the compressive loading of specimens along principal axes (with respect to fibre orientation) is considered.

In 1986, Kumar et al. reported a study of GFRP under dynamic compressive SHPB loading using cylindrical samples [76]. They found that the increase of strength with strain rate was most pronounced when loaded in the fibre direction. El-Habak agreed about the increase in strength [77], and found the rate sensitivity was more pronounced for a GFRP with a polyester rather than with an epoxy matrix. Many other authors have also observed an increase in strength with rate in GFRP composites made with a variety of matrix materials (commonly epoxy, vinyl and polypropylene) [6, 78–84], examples of which are given in Fig. 8. The modulus may increase [79, 83], remain constant [78] or reduce [76] with rate. One research team suggested that the response switches from stiff to soft above a threshold impact pressure [85]. However, in publications where data is presented it is often not clear what method was used to extract the dynamic modulus. A major problem is that elastic behaviour occurs early in the deformation when the specimen in an SHPB is not in force-equilibrium, so calculating the modulus is not straightforward and results may be difficult to justify. Most studies on unidirectionally-reinforced materials have been where the loading was in the fibre direction. However, rate-dependence has also been observed for transverse loading [84]. Significant asymmetry between tensile and compressive strength has also been found [86].

As with glass fibres, there is widespread (though not unanimous [14]) agreement that the compressive strength of CFRPs increases with rate in the fibre direction [89–93]. Some studies reported an increase in modulus [14, 90–92, 94], while others did not [89, 93]. Hosur et al. argued that high-rate stiffening arises from a combination of the effects of fibre direction, viscoelastic matrix, failure mode, crack response time, failure surface area and temperature rise [13]. Again, there is some evidence that lower failure strains may lead to a decrease in energy absorption with increase in strain rate [14]. There is also some evidence for reduced strength at high rate for compressive transverse loading [13], though this may be due to specimen edge effects producing delamination which is not seen in quasistatic loading [91, 92].

The rate dependence of composites is generally understood to be due to the behaviour of the matrix and this is certainly the case for the modulus. Studies that compare epoxy-composites with pure epoxy suggest the dynamic response of both can be described in a similar manner [79]. While many argue that the rate-dependence of yield strength follows a linear (or log-linear) relationship, others suggest a well defined transition occurs from ductile to brittle behaviour [95]. Similar arguments have been made for the stiffening behaviour [79]. However, there is typically a wide scatter in high strain rate data for which experimental repeatability may only be partly to blame [6].

Woven GFRPs have also been widely studied under high rate compression. Whereas unidirectional composites are significantly stronger when loaded along the fibre direction (where failure necessitates lateral tensile failure by 'brooming' [96]), woven materials under compression are often stronger when the woven plies are normal to the loading direction [97]. This is a geometrically-driven result, as weaves resist the lateral expansion forces produced by compressive loading. By contrast, under tensile load in the same direction, woven composites fail at similar (low) strengths as unidirectionally fibre-reinforced composites [98]. The weakest loading direction for woven composites has been found to be at ~ 45° to the plies, where global shearing can most easily occur [99, 100]. Strength again generally appears to increase with strain rate [97, 101] with a rate dependence somewhere between linear and log-linear, although there is some evidence of a weaker rate dependence at very high strain rates due to thermal softening or enhanced damage [102, 103]. Different matrix materials have been found to exhibit different degrees of rate-dependence [87, 104].

Song et al. noted that while woven CFRPs were generally stronger and stiffer at high rate, the reverse was true for in-plane compression. This was possibly due to stress

localisation at weak ply-ply interfaces. As with GFRPs, higher strengths are sometimes [105] but not always [106] observed for through-thickness loading. Ferrero et al. noticed that [±45°] CFRP layups resulted in non-linear stress–strain curves at high rates [107], while [0°/90°] combinations did not. Fibre sliding was suggested as an underlying cause of this difference: a result which could undermine orthotropic models. Nakai et al. [108] observed a slight increase in strength, but a reduction in both strain and absorbed energy, with increased loading rate in all three principal directions for [0°/90°] layups. Conversely Zou et al. reported a rate-independent modulus and increased stress, strain and elastic 'spring back' [109]. Further, these authors noted an additional complexity in loading behaviour: a 'transitional' strain rate, where failure strength and strain first decrease and then increase with increasing strain rate.

Models of the rate-dependent compression of woven composites should take account of the difference in rate sensitivity between transverse and through-thickness loading [9]. An orthotropic approach may be useful [110], though may not be enough to replicate off-axis (e.g. 45°) loading. Damage should be considered carefully [87], particularly as at high rates stress–strain curves become non-linear, indicating that damage may be initiating relatively early in the loading process [111, 112]. Furthermore, while the stitching in woven composites may not affect the overall strength or stiffness, it does appear to significantly change damage mechanisms by reducing micro-buckling and large-scale delamination in favour of much more localised 'microdelamination' [113].

Off-axis loading and shear behaviour

Because the fibres are much stronger than the matrix, composites often fail in a such a way that few fibres are damaged in the process. Reinforcement in all directions within plies is possible by alternating fibre orientations, but interlaminar failure remains largely matrix-dominated (though stitching, weaving and '3D' weaves are attempts to address this), and so for many FRPs interlaminar shear is often a likely failure mode; in certain circumstances in-plane shear may also occur. Shear experiments, particularly at high rate, may take several forms: Loading of a thin-walled cylinder in a torsion SHPB offers arguably the most 'pure' shear loading, although compression and tensile bar systems are more commonly employed, using either a shear specimen design (such as single or double lap) or off-axis fibre orientation to generate shear behaviour in a controlled manner. More bespoke experiments include 3-point bending, cylinder-torsion, rail-shear and Iosipescu shear tests. Kidane et al. offer a good review on rate dependence of shear properties [2]. They found that most (but not all) authors reported increased shear strength with rate; the in-plane shear strength for unidirectional materials, and the interlaminar shear strength for woven composites, increased with rate in all cases; but some discrepancy between results was seen for unidirectional materials under interlaminar shear and woven materials for in-plane shear.

Low rate off-axis tensile testing has been performed on composites for decades [114, 115] and are still a cause for concern [116] as clamped ends can result in induced rotation (Fig. 9 left). The use of rotating end grips [117] and/or long thin samples (length > 12 × width) [118] have been suggested to minimise these issues. Pierron & Vautrin

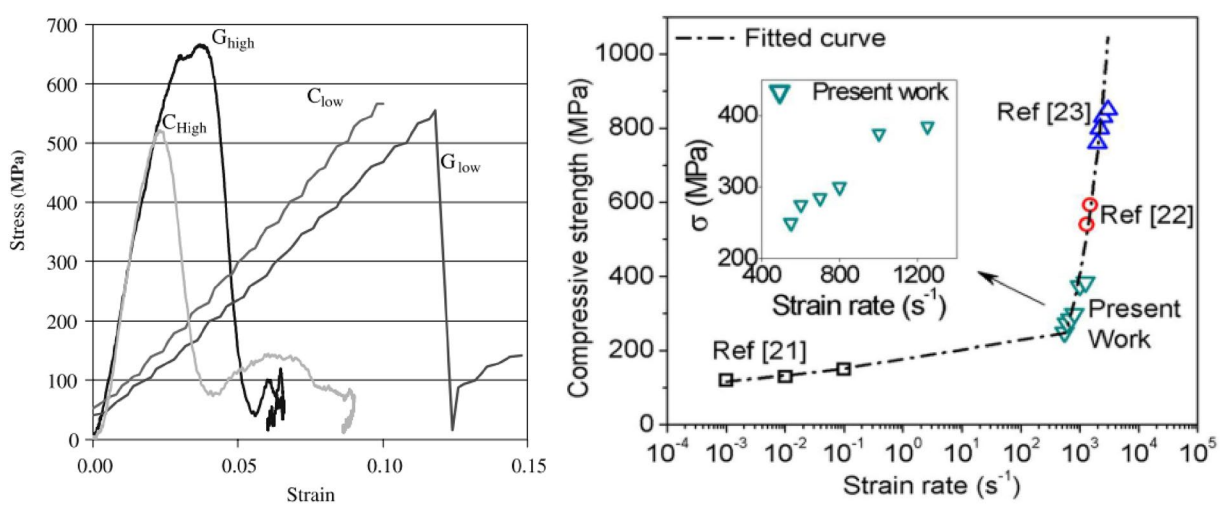

Fig. 8 Left, stress–strain plot for CFRP and GFRP at varying strain rates. From [81]. Right, average dynamic compressive strength of GFRP as a function of strain rate. From [84] (right). The numbered references in the figure are: [21]: [22, 87]: [88], and [23]: [80]

reported an increase in sample shear stress of up to 40% due to variations in the design of tabs used to grip composite specimens [119]. Oblique end-tabs promote a shear response with reduced rotation (Fig. 9 centre) [120, 121]. However, it should be noted that since the off-axis tensile test is not a pure shear test [119], additional care is required when using data obtained this way to calculate material properties.

Sayers & Harris were among the first to employ drop-weight impact testing to evaluate the dynamic shear properties of composites [122]. They observed a 30% reduction in strength between quasistatic and impact loading. The authors suggested that the high quasistatic strength is due to creep partially relieving the edge stresses between laminates. By contrast Lifshitz studied the impact loading of GFRP laminates at different angles [123], and reported that the failure stress was higher at higher strain rates, although the rate effects only become apparent during the later stages of impact. Off-axis tensile drop-weight experiments reported in 1996 found there was a decrease in shear modulus with strain rate for glass/phenolic laminates at 15°, while 45° samples exhibited rate-independent modulus [69]. The authors of this paper suggested that the reason for the difference was that the matrix behaved differently at the two loading angles. By contrast, Salvi et al. observed a slight increase in both shear modulus and shear strength of CFRP specimens with rate when subjected to a three-point bend pre-notched (mode 1 failure) test [124]. Since then a number of novel experimental tests have been developed for loading composite specimens dynamically under shear, including a hydraulic loading rig for combined transverse compression and shear [125], and a hydraulic crash machine [126] designed to deform large disk specimens. It is worth noting that damage in specimens with a small number of weft fibres can be very non-uniform under shear loading. This results in highly scattered data and 'wiggly' stress strain curves [65]. Finally, while there is little information about the effect of strain rate on the Poisson's ratio of GFRPs, one study found little rate dependence [127].

The off-axis test (Fig. 10) is relatively straightforward to perform, although sample preparation can be challenging. Some authors have been critical of this method due to (i) shear-coupling and other complications not being fully captured [1], and (ii) there being up to 30% variation in stress across a sample [128], though good lubrication to minimise specimen-bar friction can help [129].

In 1986 Kumar et al. reported compressive SHPB tests of short cylindrical specimens of a GFRP having various fibre directions [76]. They found linear stress–strain curves for 0° and 10° fibre directions with respect to the loading direction. Nonlinear behaviour was observed at larger angles. Tensile

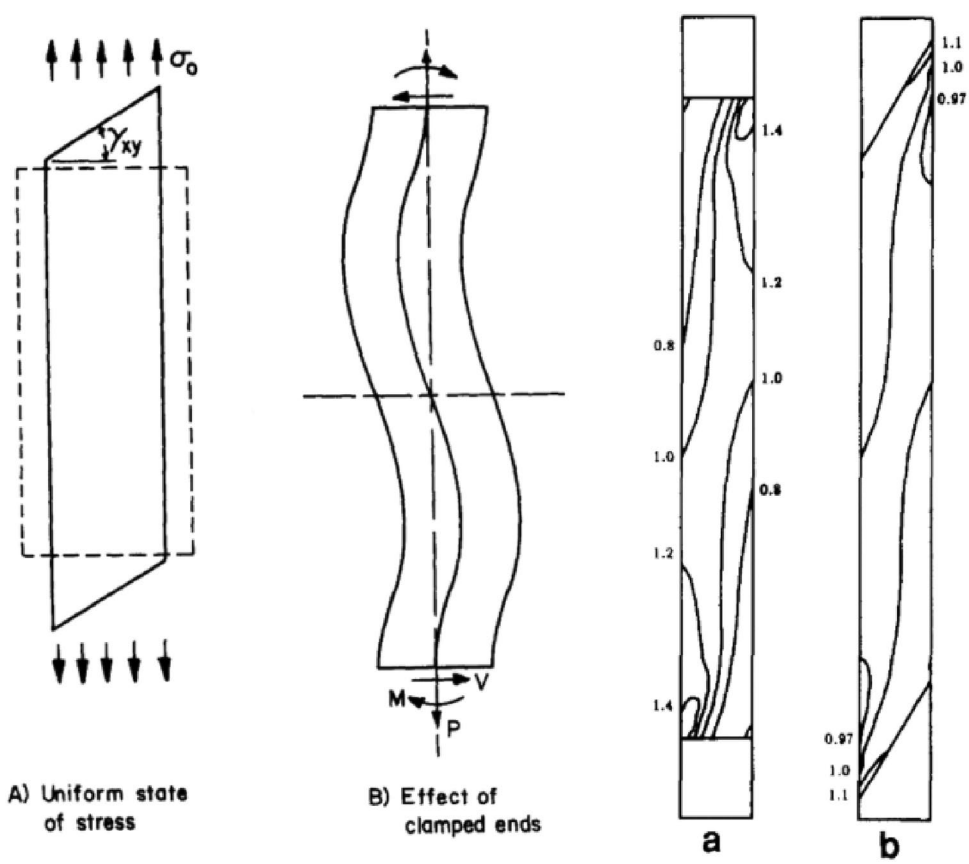

Fig. 9 Left: Effect of clamped ends on an off-axis tensile/shear test. From [117]. Right: distribution of nominal stress for specimens with rectangular and oblique tabs. From [120]

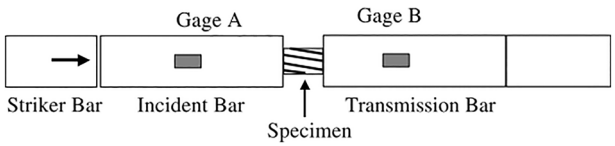

Fig. 10 Schematic of SHPB for off-axis compression test. From [130]

(lateral) splitting of fibres was the failure mechanism when the specimens were loaded in the fibre-direction, while at all other angles failure occurred by interlaminar shear. Similarly Tsai & Sun found that micro-bucking transitioned to shear failure at off-axis angles greater than 10° [130]. They also found that for off-axis angles greater than 45°, out-of-plane shear failure occurred. In their studies, shear strength increased with strain rate, while failure strain decreased. While shear strength generally increases with rate, there is evidence that the strain rate dependence varies in an unpredictable manner with loading direction [131].

For CFRPs, rate-dependence may vary depending on loading direction. For example, Hsiao et al. found that for CFRP laminates, as the loading rate was increased from intermediate to high, the in-plane shear moduli increased by 80% whereas they only increased by 18% for 30° and 45° samples [132]. However, another group of researchers [133–136] found that the ratio of transverse to in-plane shear moduli and strengths was independent of rate. In compression, the minimum yield strength can occur (via interlaminar shear) for fibres that are angled at around 60° to the loading direction [137, 138], whereas under tension the minimum occurs at 90° [139] (Fig. 11).

Several authors [138, 139] who reported increased strengths with rate noted that a Puck (Mode A) failure envelope fitted the experimental data quite successfully. Koerber et al. found that the relationship between strength/modulus and strain rate may shift from linear to a much stronger exponential relationship at strain rates above a few hundred per second [140]. Concerning failure mechanisms, Reis et al.'s study on carbon/epoxy specimens showed a transition at high strain rate from longitudinal cracking to delamination buckling failure [141]. They suggested that the transition was promoted both by extension-shear coupling effects and the viscoelastic matrix responding in a more brittle fashion.

It is also possible to obtain some insights into the shear behaviour of fibre composites from symmetric (±x°) off-axis specimens. Indeed Weeks & Sun took the view that this approach is required to avoid macro-bending issues [142]; they also cautioned that low failure strains can make acquisition of good quality data difficult. Lifshitz's dropweight experiments performed in 1976 on ±45° composites showed that while the initial response was the same as for low rate tests, the late-time (higher stress) high rate response was stiffer [123]. Later Lifshitz & Leber used an off-axis sample cut in half and bonded to create a symmetrical specimen [63]. A more recent study found that strength increased with rate, but the modulus was lower [143], and another observed greater compressive, tensile and in-plane shear strength with rate [144]. As Taniguchi et al. showed [73, 74], shear failure at low rates occurs at fibre-matrix interfaces, while at high rates cracks propagate in the matrix as well, with different rate-dependence in failure observed for different orientations (Fig. 12). Cui et al. loaded ±45° CFRPs under tension and compression [145], and also found that the strength and stiffness increased with rate. There were also changes in the failure mechanism: They found that the best fit to their results was given by a lamina-based model which considered each ply separately and included interlaminar forces and fibre orientation.

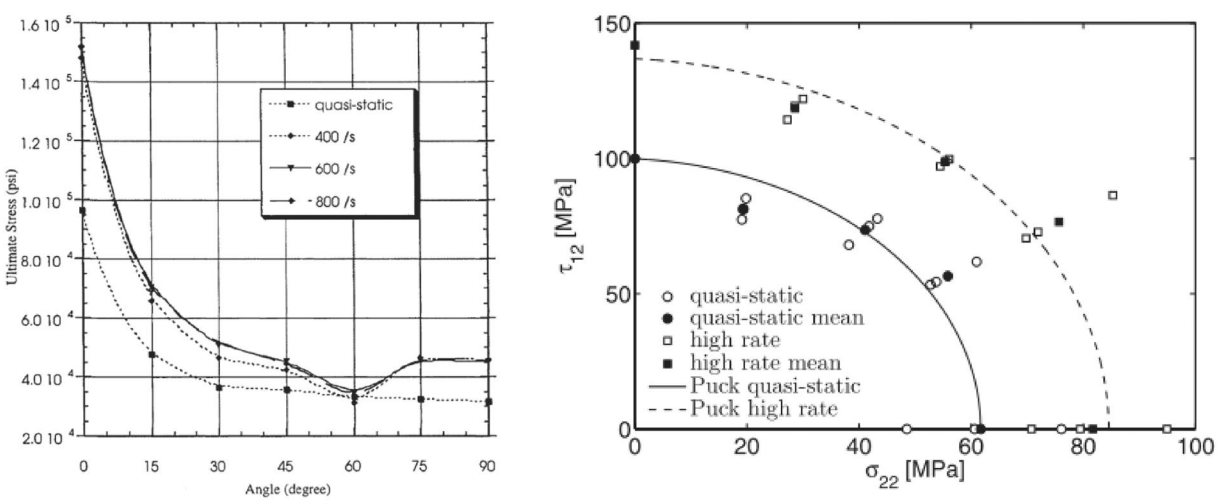

Fig. 11 Ultimate stress under compression of CFRP as a function of angle between the fibre and loading directions (left). From [137]. Quasi-static and dynamic yield and failure envelopes for tensile loading (right). From [139]

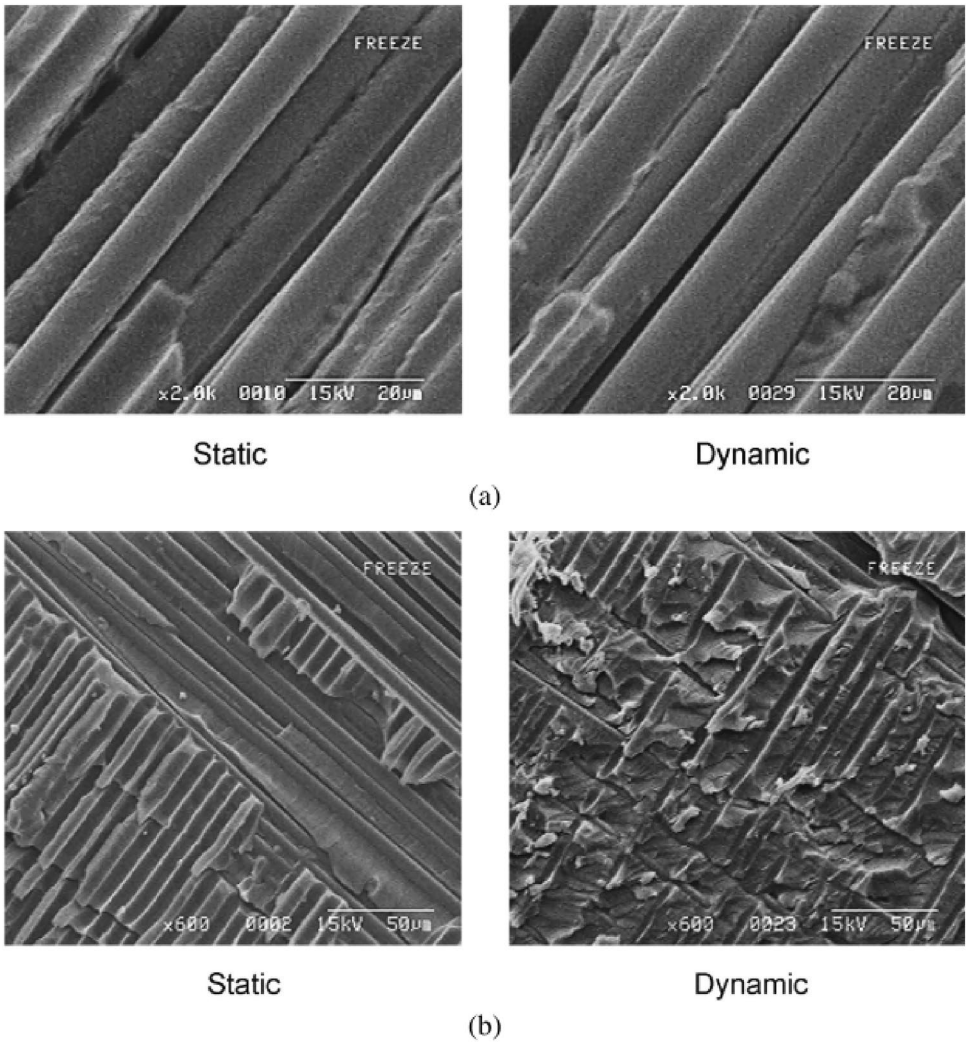

Fig. 12 Comparison between static and dynamic fracture surfaces for **a** 90° and **b** ±45° specimens. Reproduced from [73] with kind permission of Taylor & Francis Ltd (www.tandfonline.com)

Single- and double-lapped shear specimens can be loaded in compression (or less commonly in tension). For GFRP, in one single-lap study [146] a doubling of shear strength was observed between quasistatic and the fastest hydraulically driven strain rate tested. Data for CFRP is more common, driven primarily by aerospace applications: Two studies [71, 147] found the shear stress and strain increased with loading rate, while another [148] saw no difference. In contrast, a slightly lower shear stress at high rate in carbon/epoxy specimens [149], and a small decrease in through-thickness shear modulus with rate [150] have been reported. A particular issue with lapped shear experiments is the non-uniform stress distribution along the interface: Dong & Harding noted that shear strength appeared to be around 50% greater in single lap compared to double lap experiments [149, 151]. They saw fracture initiate simultaneously at both ends of the join, as normal forces were significant at these points. On the assumption that failure initiation is described by the Tsai-Hill criterion, the authors noted that the average interlaminar shear stress was estimated to be less than the true interlaminar shear strength by between 60 and 80%. Further, the shear strength of specimens with 90°/0° adjacent layers at the interface was approximately half the strength of those with 0°/0° adjacent layers.

Torsion SHPB experiments have occasionally been employed to study composites. Comparison with an SHPB torsion study of acrylic [152] again suggested that the interlaminar shear response of composites depends mainly on the properties of the polymer matrix. Under torsion loading, little rate dependence for the flow shear strength has been reported[153], as have higher shear strengths at high strain rates [154, 155]. It appears that interlaminar shear strength obtained using a torsion SHPB is lower than for single lap specimens tested using a compression SHPB. This is probably because non-shear stresses are also created in single lap specimens, resulting in an overestimate of the shear strength [2], while in a torsion SHPB test stress concentration is localised in particular fracture planes [156].

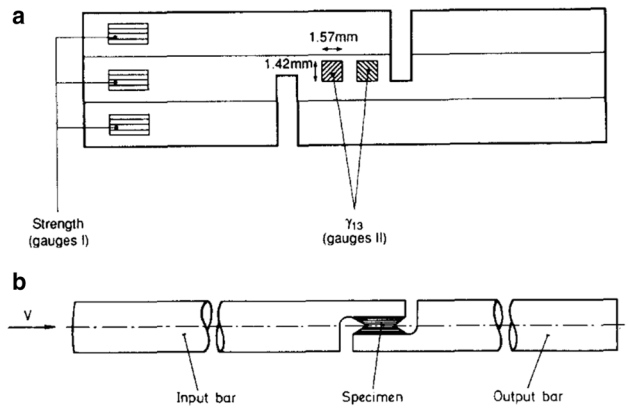

Fig. 13 Top: overlap specimen. From [148]. Bottom: notched single-overlap specimen. From [149]

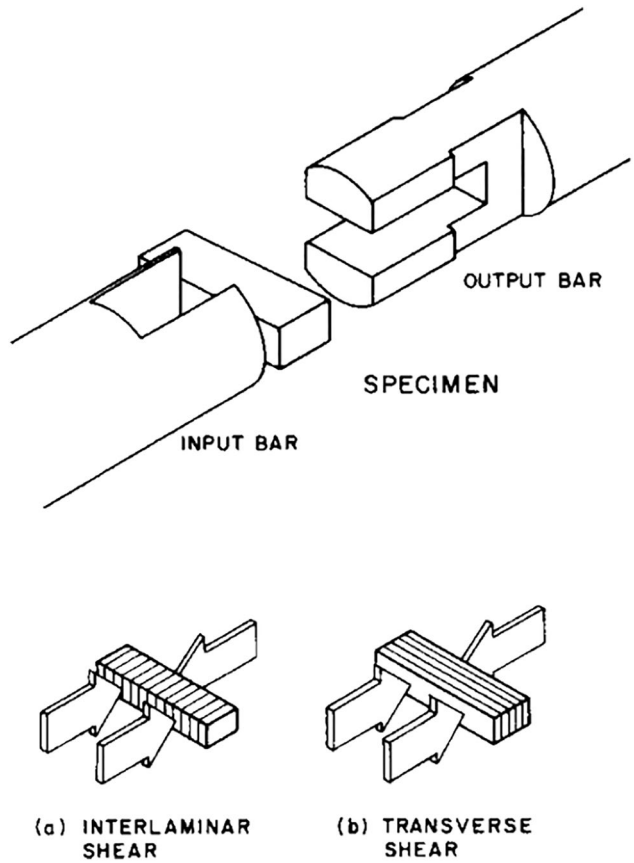

Fig. 14 A 3-point bending test. From [160]

Shear behaviour has also been investigated using several more unusual high strain rate tests. Variations on a compression-based SHPB include 'overlap' specimens (Fig. 13 top) [148], a 'notched single overlap' design (Fig. 13 bottom) [149], and an input bar-output tube design with a cylindrical shear zone in a notched specimen between the two [157]. Nemes et al. presented a novel 'punch-shear' SHPB design, which when applied to graphite-epoxy disks showed that their response depended on both loading rate and specimen thickness [158]. The experiment produced a characteristic 'knee' in the load–displacement plots which indicated the point of initial transverse shear failure, which they found increased with strain rate. This is an example of a particular loading geometry leading to a series of 'failure states' that would not otherwise be observed. Other authors have designed 3-point-bending style experiments based around an SHPB design [159]; a 3-point SHPB shear test (Fig. 14) [160] and a point-loading impact experiment [122] both indicated a decrease in shear stress (interlaminar in the former and transverse in the latter) at higher rates. In a particularly novel experiment, Fletcher et al. attempted to extract shear and transverse moduli via DICC by impacting a projectile into a short bar with an unconstrained specimen attached to the end [161].

Ballistic, Blast and Shock Loading

The previous three sections have considered dynamic loading in the simplest orientations – tension, compression and shear – which might normally constitute sufficient 'materials characterisation' efforts when studying a novel material of interest. For FRPs, however, the combination of structural and geometric effects, anisotropy and the many and varied damage and failure modes means that oftentimes, slightly larger scale experiments with more varied and complex geometries are also needed in order to obtain sufficient knowledge (and thus develop predictive modelling capability).

Concerns about the ability of FRPs to withstand ballistic impact were raised decades ago. An early review by Cantwell & Morton noted that while composites are in general strong, they are weak when subjected to localised impact loading [162]. Tests such as the one shown in Fig. 15 produce three-dimensional dynamic loading and therefore are difficult to instrument in a way which provides constitutive data useful for numerical modelling. However, they are closer to real life impacts than most laboratory tests. Three-dimensional loadings are perhaps best used as severe tests of constitutive models developed using much simpler test geometries. In addition bird-strike can be a severe problem for the engines or the pilot cabin wind-shield and is studied by a combination of synthetic and real, albeit dead, birds [163–171]. Hypervelocity impact damage to composites is of interest due to their increasing use in spacecraft, satellite bumper shields, and terrestrial armour applications [172–174].

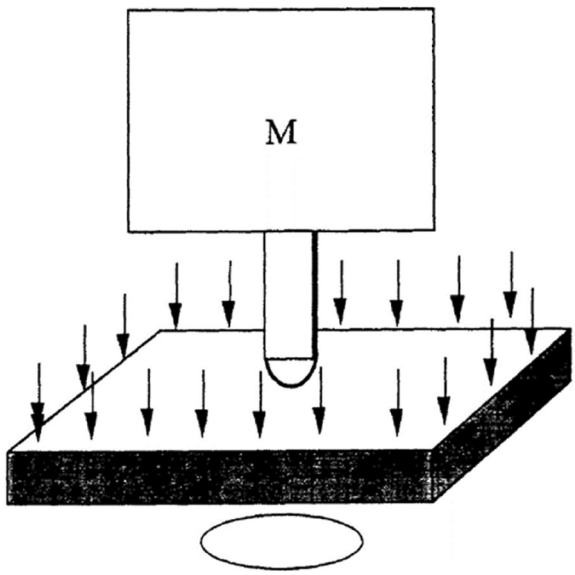

Fig. 15 Schematic diagram of drop-weight (DYNATUP) impact testing of composites. From [175]

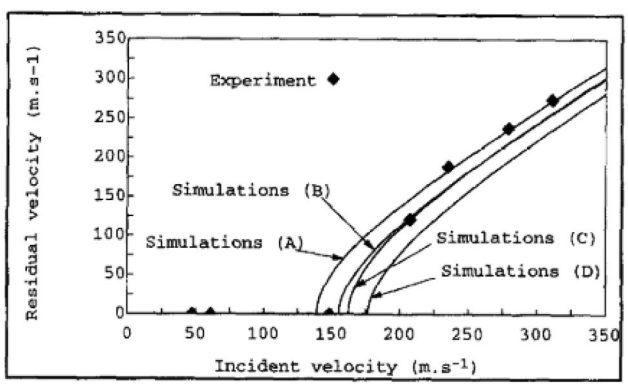

Fig. 16 Residual velocity measurements and simulations for ballistic impact. Simulations A-D are elastoviscoplastic bi-material, similar with tension and elastic shearing, elastic bi-material, and elastic respectively. Reproduced from [54] Copyright 1998 © Elsevier Masson SAS. All Rights Reserved

Several studies have employed classic 'residual velocity' ballistic tests to characterise their localised loading response at high rate: Kammerer & Neme [54, 176] fired steel balls into unidirectional composite plates, plotting the incident vs residual velocity (Fig. 16), while Justo & Marquer used Fragment Simulating Projectiles (FSPs), and found that their residual kinetic energy increased linearly with impact energy [177]. Pattofatto et al. described several iterations on ballistic loading experiments on woven glass/polypropylene [178], including sabot-backed rod impact with high-speed video displacement measurement, and 'reverse impact' in which a hollow cylindrical projectile with composite disk fixed to the front is impacted on a single Hopkinson bar. They found that the maximum load & perforation energy increased with rate, contrary to Cantwell & Morton [162].

LS DYNA has been used to model ballistic impact on FRPs by multiple authors, including Hou et al. who compared experimental results for long-rod impact with an early version of the code [179]. Lua et al.'s approach accounted for matrix cracking and strain-rate-hardening, but not delamination and disbanding failure modes [180], while Sevkat et al. took a more complex approach, assessing their model against a 22 cal impact and relying on a pair of adhered strain gauges to characterise the experimental response [181]. Budhoo et al. made use of sophisticated LS-DYNA models to predict the response to ballistic [182] and drop-weight impact [183]. Their material was described by a nonlinear orthotropic composite model which incorporated matrix cracking, brittle compressive failure, fibre breakage, tensile failure and delamination. Schiffer et al.'s analytical model appears more rudimentary, but took account of the fact that transverse shear stiffness is an important consideration [184]. Miao et al. focussed on low-velocity impact of composites of different weaves and showed distinct differences in failure modes between materials [185]: Z-weave (a 3D composite) was found to be particularly helpful at avoiding large-scale delamination, for example.

Blast loading of composite plates on their own has rarely been studied. One rare example is Mallon et al.'s work, where pre-stressed composite samples were loaded in a shock tube [186]. 3D DICC was used to track crack propagation velocity which was found to depend on fibre orientation. Most papers on blast-loading of composites have focussed on sandwich panels for blast mitigation and/or reinforcement of concrete structures with composite layers, both topics being outside the scope of this review. For more information on the current state of knowledge, see Mouritz' recent excellent review article on blast loading of composites in general [187].

Plate impact experiments have been used to investigate the shock properties of composites, although their internal structure, heterogeneity and very high fibre strength make extracting useful information challenging. Espinosa et al. used VISAR to measure the free surface velocity of woven fibre composite targets, which gave information about delamination processes occurring under the tensile load produced during the shock-release process [188]. Yuan et al. impacted composite-on-composite (with additional impedance-mismatched layers) to obtain shear strength, which (given quite a few assumptions) was shown to increase dramatically from 0.1 to nearly 0.7 GPa when the Hugoniot stress increased from 0.85 to 1.7 GPa. Tsai et al. observed no clear shock front below around 2 GPa in woven glass/polyester, and noted the difficulties in applying quasi-1D

experiments and analysis to a heterogeneous material undergoing mesoscale damage such as complex delamination and failure [189].

Joints

Joints between composite panels – both bonded and bolted – present three challenges to the understanding of the rate-dependent response of large-scale composite structures. First, they are places where the geometry is complicated, and thus often where the stresses are locally concentrated. Second, joints usually include materials such as metal pins or adhesives in addition to the fibres and matrix of the composite. Third, as the high-strength fibres which give the composite material its strength cannot cross an interface, joints are often weak regions where damage is most likely to occur. Adhesive joints rely on the strength of the polymer bond, while bolted joints require holes to be cut in the panels being joined. As a result, predicting and assessing the behaviour of joints requires a more detailed understanding of composite behaviour than is given by standard quasi-unidirectional analysis. Although the focus of this section is on joints between composite materials, insights have been obtained from the literature on joints between other types of materials. Similarly, while the high rate response is of primary interest, the quasistatic behaviour of joints is also considered for comparative purposes.

There are certain similarities between the behaviour of bonded joints and the interlaminar shear behaviour of FRP structures. However, as joints are zones of entirely fibre-free material they will have different strengths [190]. Also as joints are created some time after the curing of the composite panels that are being bonded, they are likely to be a source of weakness in the structure for this reason as well [191]. As discussed above, 'lapped' joints under load exhibit stress localisation: Zachary & Burger illustrated this issue using two epoxy-bonded photoelastic strips, dynamically loaded by the detonation of a lead azide charge (Fig. 17) [192]. The two ends of the bonded area are clearly locations of high stress, and the authors suggested that the extent of stress concentration is more intense at higher rate. The image shows that a nominally plane wave pulse results in a complex, highly non-uniform load being transmitted through the joint. Adams et al. studied a similar geometry for double-lap joints between two different materials (CFRP and steel) {Adams, 1986 #4538), and argued that stress localisation arose from the 'shear-lag effect' caused by differences in the strains in the two materials either side of the joint. Several authors have proposed that filleting (sloping) the edges near the joint can reduce the intensity of localisation (Fig. 18) {Hildebrand, 1994 #4556;Sato, 1997 #4020}. There is evidence that the stacking sequence affects the strength of bonded double-lap joints. For example, one study found that placing 0° plies on the outside was beneficial [193].

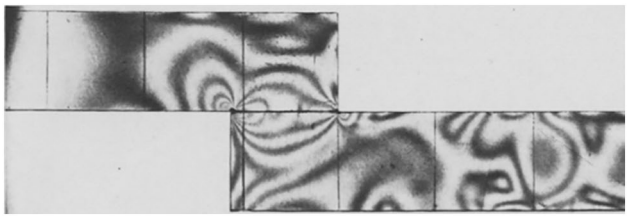

Fig. 17 Photoelastic strips subject to explosively driven plane wave loading (from the left of the image), illustrating complex stress states at the joint. From [192]

Several authors have found that the failure processes involved in the failure of joints made from composites are complex. For example, a temperature-dependent shift between brittle, stick–slip and ductile behaviour has been observed [195], and Farrow et al. found there was a significant (~ 50%) loss in strength despite the damage produced by side-on loading of joints being barely visible [196]. Side-on loading involves mixed-mode failure mechanisms which change as cracks develop [197]. All this implies that predictive models require careful design, including a focus on localised stresses [198] as well as multiple and mixed possible failure modes [199]. Various methods have been proposed for increasing the strength of bonds: (i) Avila & Bueno found that wavy lap joints could be up to 40% stronger than those that are flat [200]; (ii) Khalili et al. demonstrated that adding glass powder or short fibres to the bonding adhesive may increase joint strength [201]; and (iii) Tzetzis showed that roughening the adhered surfaces also improved bonding, although only for situations when failure occurred at the interface [202]. Roughening had no effect on 'cohesive' failure, that is when failure occurs within the bulk of the adhesive.

Methods for assessing the dynamic strength of adhesive bonds include: (i) a three-point bend test produced by means of a pendulum striker [203]; (ii) various 'ram-motion' load cells applied in a beam-bending geometry with adhesive gluing together two layers in the beam [204], and (iii) 'falling wedge' dropweights [205]. The dropweight methods have provided data indicating that higher rate tests have lower initiation energies for debonding, because they produce a smaller zone of plastic deformation than low rate tests. Rate dependent behaviour appears to depend on the type of experiment, with higher rates often resulting in increased strength (all things being equal), but with the risk that failure changes the deformation modes to ones with lower strength or energy absorption. Wu et al.'s force–deflection plots for CFRP single-lap joints indicate a factor of ~ 1.1–1.6 increase in ultimate load and energy absorption compared with static testing [206], while Tarfaoui & El Moumen's larger-scale

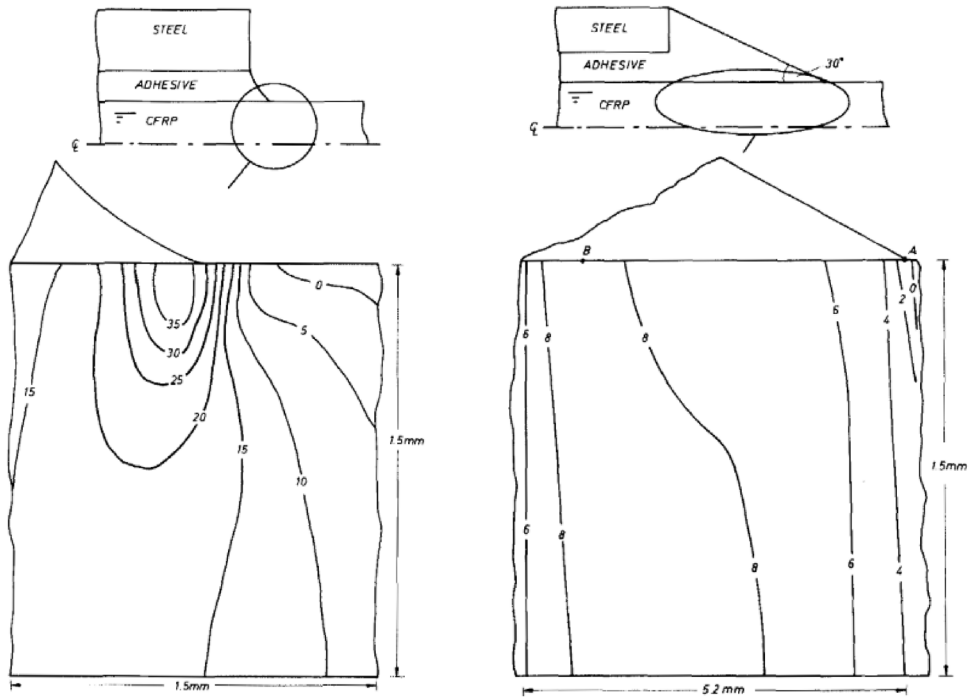

Fig. 18 'Filleting' the edges of panels in bonded double-lap joints can be seen to reduce local stress concentrations. From [194]

top-hat joints (having a balsa core with GFRP skin and stiffeners) exhibited reduced stiffness and a change in damage modes and late-time force histories at high rate [207]. In another large-scale study [208], the bonding between steel and GFRP reinforcements had a rate dependence which depended on the thickness of the composite panels. While the ultimate load capacity generally increased with rate, in one set of tests the composite underwent longitudinal tearing failure which they attributed to a non-uniform stress distribution at higher rates, which cancelled out the expected high-rate strengthening.

One study [209, 210] found that around 25µm of cyanoacrylate adhesive provided optimum strength for bonding to metals. The authors argued that due to the impedance mismatch, the SHPB is unsuitable for testing non-metallic adhesive materials in this geometry. A theoretical study modelled double-lap shear failure, and found that a thick, short, softer adhesive layer provides better stress homogeneity [211]. Janin et al., frustrated with the limited high-rate data available, decided not to perform single/double lap shear experiments and instead impacted side-on two aluminium half-dodecagons glued together [212]. This geometrical shape has joints at 15°, 45°, and 75° allowing their compression SHPB to probe multiaxial loading. A series of papers presented both experimental and modelling data for the SHPB loading of metals bonded with cyanoacrylate and epoxy [213–215]. Although the shear strength appeared to increase with rate, they found evidence that above a threshold strain rate (around 1000 s^{-1}), the failure stress and strain sharply declined to below quasi-static values (Fig. 19). They suggested that adiabatic heating of the adhesive was the reason, a conclusion that Rizk et al. also came to with regards to thermomechanical failure of joints in warm environments [216]. SHPB compression tests on cubic composite specimens with a 1 mm adhesive layer running through their centres in both in-plane [217] and out-of-plane [218] orientations suggested that while stress and modulus increase with strain rate, localised heating (which they argue is primarily damage-driven) occurred at the composite-adhesive interfaces only in the out-of-plane configuration. Further, while laminate splitting is characteristic of low-rate failure, at higher rates both delamination and interfacial separation between adhesive and adherent are important.

Bolted joints behave in an arguably even more uncertain manner, with factors such as bolt/hole size tolerance and the presence of an obvious inhomogeneity making it particularly challenging to extract general trends from experiments. Tsiang's 1984 review of bolted composite joints summarised several numerical and analytical modelling approaches [219]. They commented that such approaches are often quite conservative due to overestimation of the effects of fibre breakage when drilling holes, and noted that (i) a good understanding of through-thickness (third dimension) responses, such as delamination, was lacking, and (ii) non-destructive analysis of sub-critical damage around joints was needed to help predict failure. More recently, Pearce et al.'s experiments on bolted CFRP panels highlighted how 'simple' models struggle to replicate real-world behaviour [220, 221]. They suggested in a later paper that bolts really need a finite element (FE)

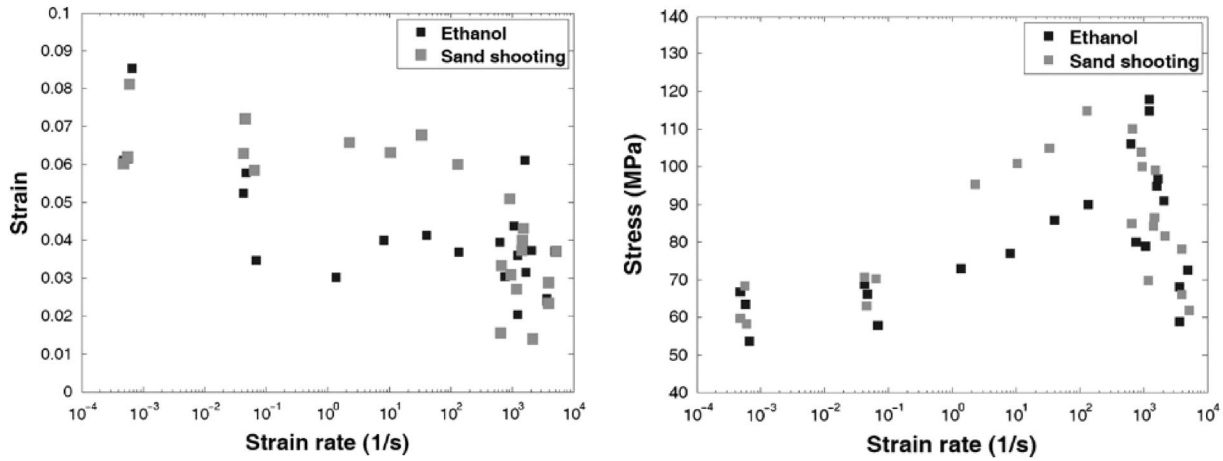

Fig. 19 Ultimate shear stress and strain of steel bonded with epoxy (for two types of surface preparation) as a function of rate. It is suggested that the sharp reduction in properties at strain rates above 1000 s^{-1} may be due to adiabatic heating of the adhesive. From [215]

approach, and delamination of plies should not be ignored [222]. Again highlighting the importance of a fully three dimensional approach, there is some evidence that preloading bolted composite joints in torsion may increase the load they can bear, for reasons that are still unclear [223]. However, inclining the bolt beyond a certain angle can weaken the joint, necessitating the use of large washers [224]; hexagonal bolt-heads should also be avoided. Further, fibre lay-up has been found to have some effect on bolted joint behaviour, as Hamada et al. noted that having 0° fibres on the outermost plies (rather than part way through) resulted in higher tensile strength [225]. In woven GFRP joints, ±45° orientation has been found to lead to more sudden failure than 0°/90°, while a sufficient distance between the pinned joint and material edge is needed to avoid unexpected failure modes involving tension and shear [226]. Recent developments include the use of micropins instead of a single large bolt [227], and an increase in the sophistication of damage and fracture analysis modelling [228].

Several studies have considered the rate-dependence of bolted joint behaviour in the regime between quasistatic and medium rate loading. Li et al. suggested that joint strength was a minimum for impact velocities of around 5m/s in riveted composite joints [229]. Heimbs et al.'s study suggested that while single-lap shear with one bolt showed little to no rate dependence [230], a single lap shear with two bolts did show increased strength and energy absorption at 10m/s due to a change in failure mode from net tension to "extensive bearing and pull-through failure". Another study also noted a change in damage mode between quasistatic and 2m/s loading [231], but while they found that the failure stress increased, the absorbed energy *decreased* (presumably due to rate-dependent stiffening).

Little information about the high-rate loading of bolted composite joints has been published in the open literature. From the data that is available, it appears that whether their strength increases or decreases with loading rate depends on the specific geometries and materials involved. Ger et al. found that for carbon and hybrid fibre composites, the bearing strength decreased with rate [232]. They also reported: (i) a more pronounced decrease for pinned joints which lacked side-clamping pressure; (ii) a smaller reduction for double lap compared to single lap joints; (iii) tensile failure due to high stress concentration at the joining hole was what governed the rate dependent behaviour; and (iv) their bonded joints were stronger at high rate. VanderKlok et al. studied metal and composite plates that were bolted together [233]. While generally stronger at high rate, the rate dependence appeared to depend strongly on the ratio 'e/d', where e is the distance from the far edge of the plates to the bolt centre, and d is the bolt diameter. A ratio of 1 resulted in slightly lower strength at high rate, 2 a slightly higher strength, and a ratio of 3 produced a compound structure that was much stronger under high rate loading than quasistatic. A combination of failure modes, inertial effects and load transfer rate were suggested as underlying causes of the variations observed. Finally, Wang et al. applied tensile loads to GFRP single-lap bolted joints, and found that both strength and stiffness increased at higher rate [234].

Underwater Loading

Use of FRPs in marine applications date back as far as World War 2 [235]. They were introduced because (i) they are lighter, (ii) they are non-magnetics (and hence are particularly useful in minesweeping), (iii) metals corrode in seawater, and (iv) wood is eaten by marine organisms. To

date, FRPs have been used for "hulls, bearings, propellers, hatch covers, exhausts, topside structures, radomes, sonar domes, railings, vessels of all types, valves and other subsea structures [235]." 'E-glass' is most commonly used, with occasional use of the stronger S-glass (also known as R-glass or T-glass). The much more expensive carbon fibre is rarely seen in marine applications, in contrast to aviation where high strength-to-weight ratio requirements often outweigh material cost considerations. Marine application presents two unique challenges beyond that hitherto discussed in this review: FRPs can be subject to mechanical changes when submerged, and underwater loading can involve phenomena such as bubble collapse and much longer duration loading pulses than typically seen on land or in the air.

Submerging composites in water (whether pure, tap, salt or sea) changes their mechanical properties, most notably through plasticisation and softening of the matrix [236] – although Wang et al. noted that seawater also strongly degrades adhesive carbon–carbon bonding [237]. Dynamic mechanical analysis (DMA) data for glass/plastic confirms that changes in mechanical properties (principally those of the polymer matrix) which occur from prolonged submersion may not be entirely reversed by repeated drying [238]. Woldesenbet et al. [239] claim plasticisation by water increases the ultimate stress in carbon/epoxy, though not at high strain rate when submersion takes place at higher temperatures (Fig. 20). Conversely Yin et al.'s glass/polyethylene composites generally lost strength after being immersed in seawater [240]. They found the immersion temperature affected the result: hotter baths led to a greater loss in flexural strength, but a less pronounced reduction in tensile strength. Two other studies, on glass/vinyl ester [241] and pure epoxy [242] found that degradation due to moisture was worse for low rate loading; the effects being reduced when loads were applied in the (glass) fibre direction. The effect of moisture on bonded joints is also important to understand: Ferreira et al. found that bonded composite joints can lose around 30% of their static strength after a few weeks in water [243].

Replicating underwater blast loading in the laboratory is challenging, for while it is possible to apply dynamic loads whose peak is representative of a full-scale event, the loading duration is necessarily shorter. This is particularly important for composites for which the total impulse – not just the peak strength – is an important factor in the production of damage. Mouritz and co-workers have published a series of papers on submerged charge blast loading of composite panels [244]. They showed that while stitching reduces delamination damage, stitches acted as stress concentrators which increased local damage at the point of failure [245]; defects arising from particular lay-up techniques significantly affected shock strength [246]; and material degradation from repeat loading only became apparent due to serious delamination or fibre damage, not matrix cracking [247]. One conclusion from this series of studies was that data obtained from simpler quasi-static 4-point bending tests could be extrapolated to the blast loading case using a simple rate-dependence relationship [248]. Mouritz' recent review [187] of blast loading composites concluded that comparing the many studies that have been performed is difficult mainly due to differences in experimental methods. In particular, information is lacking about repeat loading (critical for underwater cavitation) as is the response to near-field (high stress) blast.

Rather than use an open-tank blast design, LeBlanc & Shukla instead employed a conical shock tube (Fig. 21) with triaxial strain gauges mounted on a cylindrical specimen which can be either air- or water-backed [249]. Both the water and the composite specimen were modelled with LS DYNA. Subsequent tests considered curved panels [250] and pre-stressing of samples [251]. In the studies reported in their final paper, they varied both the curvature (bowing

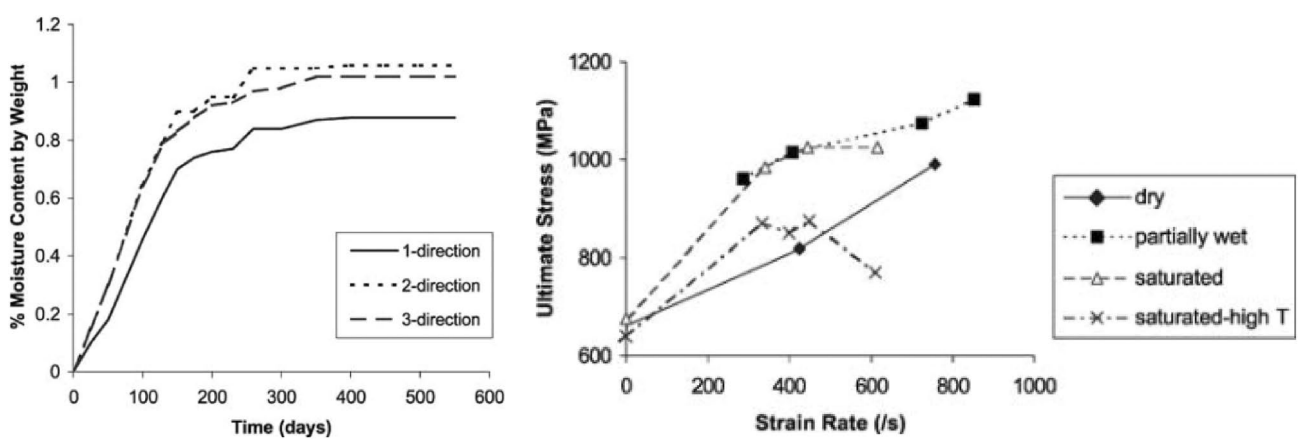

Fig. 20 Moisture absorption of ca. 6 mm diameter carbon/epoxy cylinders immersed in distilled water at room temperature (left), and ultimate stress vs strain for different moisture conditions in the fibre direction (right). From [239]

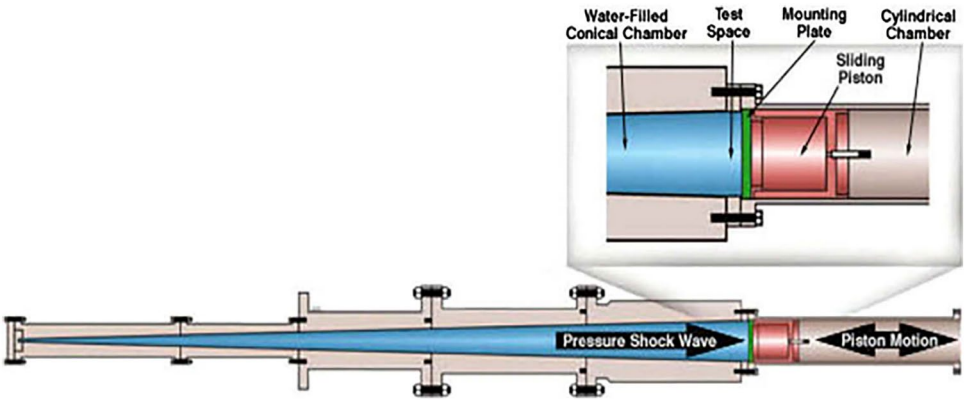

Fig. 21 Conical shock tube schematic with expanded detail of piston. From [249]

towards the loading direction) and the thickness, showing that more acutely curved specimens are stiffer and buckle less [252]. More recent large-tank explosive tests have involved (i) cantilevered plates [253], and (ii) the analysis of the resistance to the formation of holes during through-thickness penetration by considering the energy required to initiate fibre rupture [254] (where the Von Mises strain exceeded the ultimate elongation of statically loaded samples twofold). Rolfe et al. performed much larger scale blast loading tests both under water and in air with several kgs of explosive material [255]. Gauch et al. showed that polyurea coatings help reduce damage from underwater blast loading but also increase strain during early time deformation [256]. Ren et al. considered sandwich panels [257]. In most cases, the primary aim was the comparison of experiment with (and thus validation of) various modelling approaches.

Due to the geometric complexity (and more direct real-world application) of underwater blast, it has been a particular focus of modelling efforts over the past decades. Early publications were mostly reporting analytic studies of fluid–structure interactions, such as those involving submerged composite cylinders [258] and attempts to replicate underwater explosive loading (UNDEX) with a simpler equivalent system [259]. Gong & Lam published a series of papers assessing the transient response of composite submersibles to explosive loads, using some coupled equations and an FE model [260]. Structures modelled included a floating composite ship section [261], and a layered beam [262]. Some structural damping and stiffness effects were included. Motley et al. modelled in 3D the shock response of composite marine structures to underwater blast [253]. They noted how more flexible panels resulted in better energy transfer across the plate, a macro-scale structural effect rather than a material property. The authors noted the comparative difficulty in predicting brittle composite failure as opposed to ductile deformation of metal components. The systems that have been modelled include: (i) sandwich panels under blast load [263, 264] (the authors ignored certain complex phenomena such as small amplitude, high frequency oscillations); (ii) numerical modelling of a complete submarine hull subject to stand-off explosion [265, 266], and (iii) a peridynamic thermomechanical model of shock-loaded marine composites [267].

Replicating underwater blast at full-scale necessarily involves relatively large, spherically symmetrical (as opposed to 1D) experiments, which are made more challenging if explosive charges are used. It is therefore sensible to attempt to replicate blast loading conditions using pressurised inert gases. A small number of in-house designs of experimental apparatus to achieve this have been reported in the past few decades. One example is Espinosa et al.'s design for performing shock experiments in water [268, 269]. They used a gas gun to launch a flyer that then impacted a piston of smaller diameter, thereby driving a shockwave though a water-filled tapered tube to load a circular disk-shaped composite specimen. The diagnostics they used included high-speed photography, shadow moiré, and pressure transducers positioned along the length of the edge of the water tank. Wei et al. later modelled these experiments, noting in particular that delamination was highly rate-dependent [270]. Georgia Tech's Underwater Shock Loading Simulator (Fig. 22) is similar, and uses measurements of deflection and calculation of absorbed energy (using Abaqus/Explicit models) as the main analysis tools. Experiments performed include testing various sandwich panels [271, 272], the response to blast of cylindrical composite structures [273–275] and hybrid metal-composite plates [276].

A smaller-scale apparatus was used by Schiffer et al. to test circular composite plates [277]. Iterations of the design allowed for a variety of different composite specimens to be assessed and compared with models. Initial experiments produced minor shear failure in air-backed specimens loaded up to 10 MPa [278]. Double-skinned specimens with water in between [279] and sandwich plates [280] were also tested. Making the shock tube out of a transparent material allowed high-speed photography of the water during dynamic loading. This facilitated analysis and comparison with modelling of cavitation activity, additional (re)loading and other

more complex fluid dynamic interactions as the specimen plate deformed [281]. Researchers in China have recently conducted similar experiments [282, 283].

Dropweight experiments where composite plates were loaded on the surface of [284] or immersed in [285] water have also proved insightful. Owens et al. reflected on the importance of fluid–structure interaction (FSI) effects in relatively dense fluids such as water [285]. 'Added Virtual Mass Incremental' factors, that is to say the ratio of kinetic energy in water to that in the plate, were on average eight times greater in the air backed case and nearly four times higher in the water-backed case. The authors noted that these factors are significantly greater than the typically quoted figure of 1.4 for steel plates submerged in water. A subsequent paper by Kwon [286] expanded on this to explain that FSI has a significant bearing on structural dynamic behaviours such as frequencies, damping, and magnitudes thereby strongly affecting the failure of composite structures under water. In other words, the modest difference in density between water and composite panels strongly reduces the 'effective' loading stress applied to a composite panel if it is immersed in water on both sides, compared to the same panel backed by air.

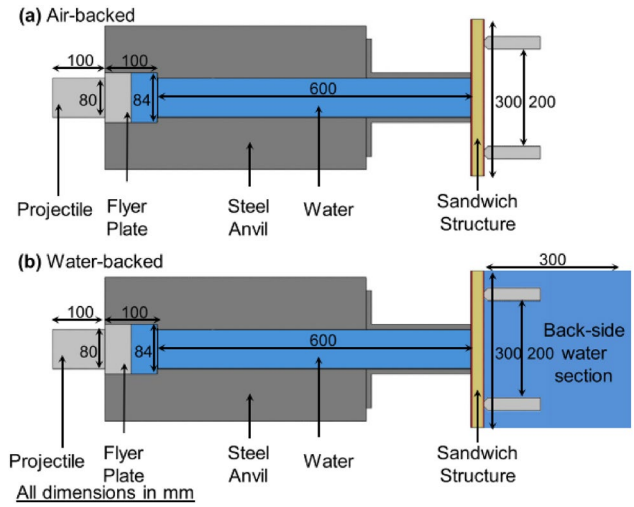

Fig. 22 Georgia Tech's Underwater Shock Loading Simulator (USLS) for measuring the response of various structures to underwater impulsive loading. From [274]

Table 2 Typical values of the energy absorbing capability of various continuous fibre composites for different failure modes. From [162]

Failure mode	Material	Typical fracture energy ()kJ m^{-1})
Splitting	Type II CF/epoxy	0.1–1
	AS4/PEEK	3.8
Delamination	T300/epoxy	0.1
	IM6/PEEK	2.2
Transverse fibre fracture	Treated CF/epoxy	20
	Untreated CF/epoxy	60
	AS4/PEEK	128
Fibre pull-out	CF/polyester	26
	CF/bismaleimide	800
Debonding	CF/epoxy	6

Damage, Failure and Energy

The previous sections have largely discussed the rate dependence of deformation through the lens of traditional mechanical analysis approaches. In this section, further consideration is given to the more FRP-specific processes occurring during deformation such as damage modes and energy absorption, which are not necessarily captured if we limit our assessment to that of failure stress and strain. As noted in the introduction, fracture mechanics in composites is a substantial area of research in itself, and so not something this review has space to assess in detail.

There are many possible damage and failure processes in fibre-reinforced composites. The particular failure process that occurs in any given scenario will depend on a number of factors including the loading rate, specimen shape and size, fibre weave, layup, pre-existing flaws or damage, temperature, fibre and matrix properties and interactions between them. As a result, in many cases 'standard' materials characterisation tests may not be sufficient to fully characterise and predict behaviour. Cantwell & Morton tabulated the energy required for various failure modes in quasistatic loading (see Table 2), highlighting the much greater work required for fibre fracture and pull-out compared with splitting, delamination or debonding [162].

The physics of the damage mechanisms in composites is surprisingly complex. Localised impact results in a delaminated area which depends on impact force [287], for example, while adding stitches between plies reduces the risk of structural damage leading on to catastrophic failure but at the expense of degraded in-plane mechanical properties [288]. Interactions between the physical constituents of damaged materials are still poorly understood. Kendall proposed that 'structural dislocations' (small voids and cracks) might function to arrest the propagation of damage by cracking, in a manner similar to dislocation-driven work-hardening in metals [289]. The propagation of different types of damage can also differ quite significantly: A three-point bend configuration in a modified Kolsky bar showed that mode II cracks extend much faster crack than mode I [290]. Lee et al., however, found that in unidirectional CFRPs, the

crack speed was faster for mode I than for mixed mode I & II [291].

Several studies have focussed on fibre-matrix interactions, often by using simplified model systems. In 1980, Mandell et al. performed indentation tests to assess fibre-matrix bond strength, which involved compressing a fibre or region of fibres on the surface of a polished specimen [32], then removing the indenter and visually assessing debonding. Bi et al. studied the initiation and propagation of cracks at the fibre/matrix interface of a model aluminium/epoxy system [292], and found that the dynamic interface strength and toughness were considerably higher dynamically than the quasistatic values; Li et al. observed similar results, which were also strongly dependent on surface roughness [293]. Gradin & Bäcklund made a macroscopic physical model of fibre debonding by setting epoxy around a steel cylinder, which they then pulled out [34], observing that longer cracks at the interface grew faster. Tamrakar et al. devised a SHPB-style single fibre and micro-droplet pull-out test, which they claimed was the first such study to be performed at high rate [294].

Methods for tracking damage evolution in real-time during an experiment are being developed. Mahmood et al. coated glass fibres with graphene oxide (which is piezoresistive) in order to record strain in real time [295] – with the added benefit that the graphene oxide layer improved the flexural strength by 23% and the interlaminar shear strength by 29%. Minnaar developed a non-contact crack detection method [290] which consisted of a series of four laser interferometers that measured the displacements of the surface, allowing the degree of delamination to be determined. Woo & Kim [296] employed acoustic emission and wavelet analysis to SHPB experiments to find particular frequency ranges which may correspond to different damage mechanisms such as matrix fracture, fibre-matrix debonding, fibre pull-out, and fibre breakage. Riccio et al. investigated delamination buckling and growth phenomena in stiffened composite panels under compression [297] by embedding optical fibres in the skin of the panels close to an artificial delamination.

Assessment of damage and failure in recovered samples post-experiment is most commonly performed using optical and electron microscopy, although an increasing diversity of diagnostic tools are beginning to be employed. Duchene et al. recently reviewed the non-destructive techniques that are used for the assessment of mechanical damage [298]. Acoustic emission and acoustic inspection are becoming increasingly widely used, although it is difficult to differentiate between different types of damage, and high attenuation in heterogeneous composites makes it difficult to use these techniques on thicker specimens. DICC optical techniques, as mentioned elsewhere in this review, can be used to measure full field strains at a specimen surface in order to obtain deformation maps. X-ray radiography and tomography are better for smaller specimens but cannot be used to study very small cracks. Infrared thermography, shearography using lasers, electrical resistance and eddy currents have also been used with varying success. Wu et al. used a pulse echo reflector technique similar to ultrasonic imaging, and found that they were able to detect hardly-visible impact damage and pre-failure delamination within a composite [287]. Saeedifar et al. combined passive and active acoustic methods to assess non-visible damage [299], while Xue et al. used both acoustic emission and X-ray microtomography to observe damage due to a compression stress of 60 MPa in a specimen whose yield strength was more than twice that [300]. Russo claimed that it was possible to detect and quantify the damage to GRFP structural elements by measuring their elastic response and inputting this into an FE model [301].

Various authors have shown that strain rate has an effect on the stress–strain behaviour, much of which is attributed primarily to the strain rate sensitivity of polymer matrix materials. For example, Tasdemirci & Hall [112] observed a linear relationship for composites compressed under quasistatic conditions, but not for higher rate loading. Griffiths and Martin also observed an increase in nonlinearity with rate [302]. Departure from linearity indicates a change in modulus due to damage, suggesting that despite strength being observed to increase with strain rate, the same may not be true for the damage threshold. Indeed damage mechanisms may vary with rate as well as with loading geometry, specimen structure and other variables. For example, Werner & Dharan observed that the density of interlaminar cracks increased as the strain rate was increased [160]. Several authors have observed a change from splitting (or delamination) to fragmentation in composites loaded using compression SHPBs as the loading rate (and stress) increases [13, 94]. Taniguchi et al. impacted hollow composite tubes side-on, and observed differences in the fracture surfaces [303]: At high rates, failure appeared to occur mostly within the matrix, rather than jumping between the matrix/fibre boundaries (Fig. 23). Small changes in the loading configuration can have surprising effects, such as Minak et al.'s discovery that for composite cylinders impacted at low velocities, preloading the specimen in torsion didn't noticeably affect when damage first initiated, but did lead to damage propagating

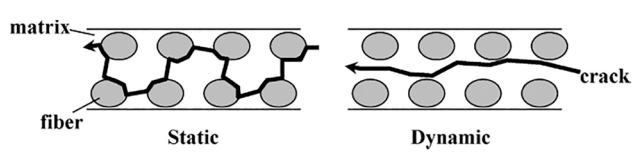

Fig. 23 Comparison of the fracture surface behaviour between static and dynamic tests, as observed by Taniguchi. Reproduced from [303] with kind permission of Taylor & Francis Ltd (www.tandfonline.com)

much more readily thereafter [304]. Tsai & Chen investigated the nonlinear rate-dependent properties of CFRPs using micromechanical analysis [305]. As expected, they found experimentally that CRFPs stiffen as the strain rate increases, and they attributed this observation entirely to the epoxy matrix rather than the fibres. They measured the properties of both the epoxy and the composite, and then compared the results to their micromechanical model.

Failure modes, too, may change with strain rate. For example, Gama et al. found that when they compressed unidirectional and woven glass/vinyl, kink bands were formed at both quasistatic and SHPB rates [6]. However, there was much more interlaminar delamination at high rates implying tensile failure of the plies perpendicular to the loading direction. Failure also occurred on multiple planes at high rates, but for quasistatic loading failure occurred only in the maximum shear plane. One driving factor behind these changes is that damage processes are not instantaneous, but take time to nucleate and grow. Energy is also required. Accordingly, various attempts have been made to model strain rate dependent damage behaviour [306–308]. Lataillade et al. investigated this experimentally by using a strain-arrest tensile SHPB apparatus to load ± 45° off-axis (symmetrical) specimens to better understand damage propagation [309]. Fibre-matrix unsticking appeared first, before microcracks coalesced between fibres, and an initial elastic region was followed by an 'anelastic' plateau in the stress–strain plots. The authors argued that at higher rates, damage initiation is delayed, and reduces the rate of propagation.

At very high rates, adiabatic heating of the viscoelastic matrix during compression may occur, and there is evidence that this may lead to a significant drop in strength above a threshold rate [213–215]. As a result of these observations, Li & Ghosh recently developed a continuum damage model which includes adiabatic heating so as to improve understanding of high strain rate impacts [310], although their model does not appear to replicate the dramatic strength reductions that some researchers have observed. Tarfaoui et al. measured the deformation, damage mode and temperature simultaneously of deforming GFRPs both quasistatically and at high strain rates in an SHPB [311]. The greatest local temperature change they observed was 219 °C, with hot zones localised at damage sites, suggesting that heating is not just due to the viscoelastic response of the matrix.

As discussed in previous sections, the yield and ultimate strengths of FRPs tend to increase with strain rate in most circumstances. However, there is much less agreement about the effect of strain rate on modulus and failure strain, in large part as a result of to the difficulty in accurately and reliably measuring these parameters at high rates. For these reasons, we will discuss a collection of papers which considered the issue from the point of view of energy absorption. Several studies reported an increase in toughness with rate: (i) Adachi et al. evaluated the interlaminar dynamic fracture toughness of unidirectional CFRP laminates using "end notched flexure" specimens in an SHPB to drive mode II delamination [312]; (ii) Kuhn et al. compressed double edge notched specimens of various sizes in the fibre direction [313]; and (iii) Leite et al. performed a four point bending investigation of the interlaminar fracture toughness of a CFRP [314] (Fig. 24). Compression of unidirectional GFRPs has been shown to result in similar increased energy absorption before failure [83], with both matrix and fibre failure modes thought to contribute [80].

However, even for simple SHPB compression experiments, changes in failure mode – particularly for carbon composites – have been seen to significantly reduce failure strain as strain rate is increased, leading to a decrease in toughness with rate [81]. Taniguchi et al. conducted side-on impact studies of hollow composite tubes in which the fibres were oriented at either 0° or ± 45° [303]. They found that the energy absorbed increased with strain rate for 0° fibre specimens, but remained constant for tubes where the fibres were arranged at ± 45°. Furthermore, the effect of strain rate on energy absorption changed after onset of damage: before damage occurred, the energy absorbed increased with rate, but after damage initiated the energy absorption decreased as the rate was increased.

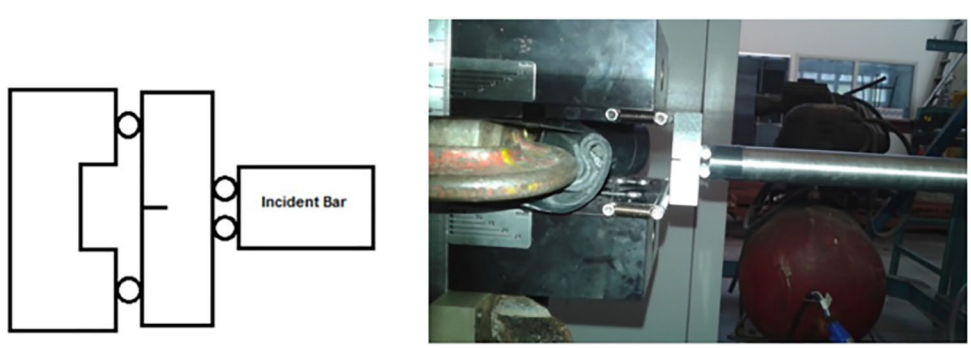

(a) Schematic assembly (b) Real assembly

Fig. 24 Schematic and photograph of the experimental setup for four-point bending SHPB experiments. From [314]

Mesoscale structure, as well as rate, can affect the energy absorption properties of a composite. Daryadel et al. found that energy absorption depends on structure, with glass fibres surrounded by graphite fibres providing the highest specific energy absorption and highest ultimate strength [315]. Interestingly, observations made with a high-speed camera showed that the specimens were not visibly damaged at the peak load, but the surface started to shatter a few microseconds afterwards. Tarfaoui et al. used energy balance to quantify the energy dissipation during SHPB tests, and found that although stitching between plies did not increase the damage initiation strength, it did increase the fracture energy for crack propagation as z-direction fibres help to prevent delamination [316]. As an example of very specific rate sensitivity in dynamic response, Yasaee et al. investigated the strain rate dependence of mode II delamination resistance using three-point end notched flexure specimens with and without z-pins (i.e. fibres in the z-direction) [159]. Unsurprisingly, z-pins increased the delamination toughness as they specifically reinforce the dominant interlaminar shear failure mode. More interestingly, a significant increase in toughness was observed at higher rates as the z-pins failed by shear rather than pull-out. Indeed the balance of work done between particular damage modes is not necessarily obvious. Simulations [273] suggest that delamination might contribute only 20% of the overall fracture work and ~ 5% of total energy dissipation – but is the driving force of other failure modes such as intralaminar cracks – while friction between cracked surfaces could account for a similar amount of work done as fracture and strain.

Repeat Loading

One of the biggest concerns about using FRPs in many applications is the extent to which degradation in structural properties can accumulate without any obvious signs of damage or failure. Fatigue testing (a subject beyond the scope of this review) offers some insight, but at high strain rates, one subject of particular interest is the extent to which a single loading event – such as a bicycle crash or bird strike on an aircraft – might lead to a reduction in residual strength or toughness.

Because deformation in composites is always accompanied by damage (which is irreversible and cumulative) an applied load which does not cause yield or visible damage may reduce the ability of a composite to withstand a second loading event. Some low-rate studies have addressed this concern, but the rate dependence of the effect of multiple loading is difficult to assess due to the experimental difficulty of applying a load at very high rate in a stress- or strain-limited manner. For example, Li et al. found that the damage produced by repeated low velocity impact increased with successive blows [317]. Strength has also been found to decrease for samples which have been previously loaded [162, 318]. There is some disagreement about the load required to trigger a reduction in strength: Cantwell & Morton observed a roughly constant decrease in residual strength with impact energy (Fig. 25); Oleg et al. argued that a threshold load was required [318]; and Mouritz' underwater shock loading experiments [247] suggested that fatigue strength only noticeably decreases once delamination or fibre damage has occurred – minor amounts of matrix cracking appeared to have little effect. Bolted joints are also weaker under cyclic loading, with one study recording a 63% reduction in strength [319].

Tarfaoui et al. studied the residual strength of damaged GRFP tubular structures, 55 mm diameter with 6 mm wall thickness [320]. The resulting damage was assessed using both ultrasonic transducers and by injecting UV sensitive penetrant into cut sections – with the latter technique showing the extent of the damage to be around ten times larger than the former suggested. They found there was a threshold impact energy of around 3 J for damage to appear at the surface, a rapid increase between 3 and 5 J due to macroscopic delamination, and then a more gradual rise with energy as cracks propagated within the debonded plies (Fig. 26, black data). The pre-damaged tubes were then subject to an increasing external hydrostatic pressure until the tubes imploded (Fig. 27), revealing a relationship between failure stress and pre-damage. Notably, they found that the direction of the damage mattered: radial delamination had little effect on implosion resistance, but there was a significant reduction in failure stress at slightly higher impact energies where intralaminar cracks also occurred (Fig. 26 orange data). It is important to note that this result is likely to be highly specific to this particular set of loading conditions so that

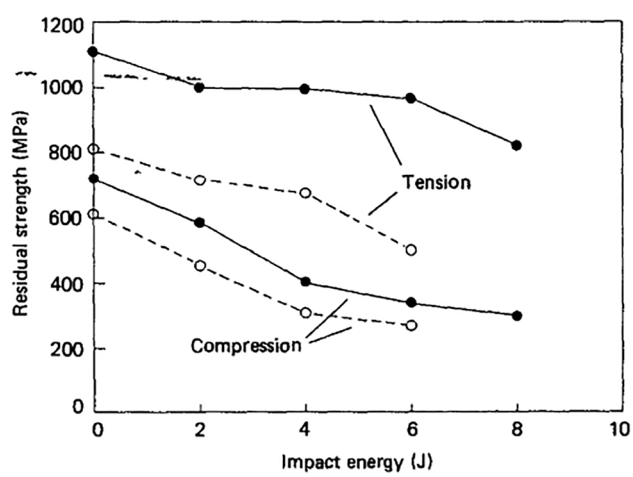

Fig. 25 Residual strength of composites with two types of fibre (solid and open circle data points). From [162]

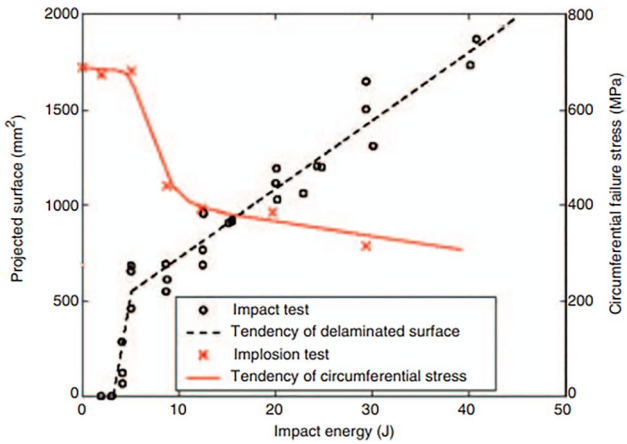

Fig. 26 Relation between delaminated surface area and impact energy due to initial impact loading (black data and circular points), and subsequent failure stress during underwater implosion of the pre-impacted specimens. From [320]

a particular type of damage from the first loading scenario leads to a particular failure mechanism in the second.

Specimen Geometry and Damage Localisation

In the previous sections we have considered the response of an FRP specimen to dynamic loading under a wide range of conditions. Almost exclusively, a single specimen geometry was chosen and tested in each study – and so comparisons between different experiments, materials and authors are required to build a picture of how different deformation phenomena, damage and failure modes can arise under different loading conditions. For this final technical section, we review differences in response observed when specimens of varying geometry are compared under similar loading conditions, and consider whether strain rate effects may be different for 'uniform' specimens (which are the subject of most studies in the literature) than for those where specimen geometry leads to spatially localised stress concentration .

As composites are technically structures rather than materials, their dynamic properties are a combination of intrinsic 'material' and extensive 'structural' responses, as evidenced by the studies highlighted in this section. Careful consideration must therefore be paid to all possible deformation mechanisms, some of which may not arise through oft-used testing procedures sufficient for characterising more standard materials. This is a particular challenge at high strain rates, where non-equilibrium and wave effects have to be taken into account.

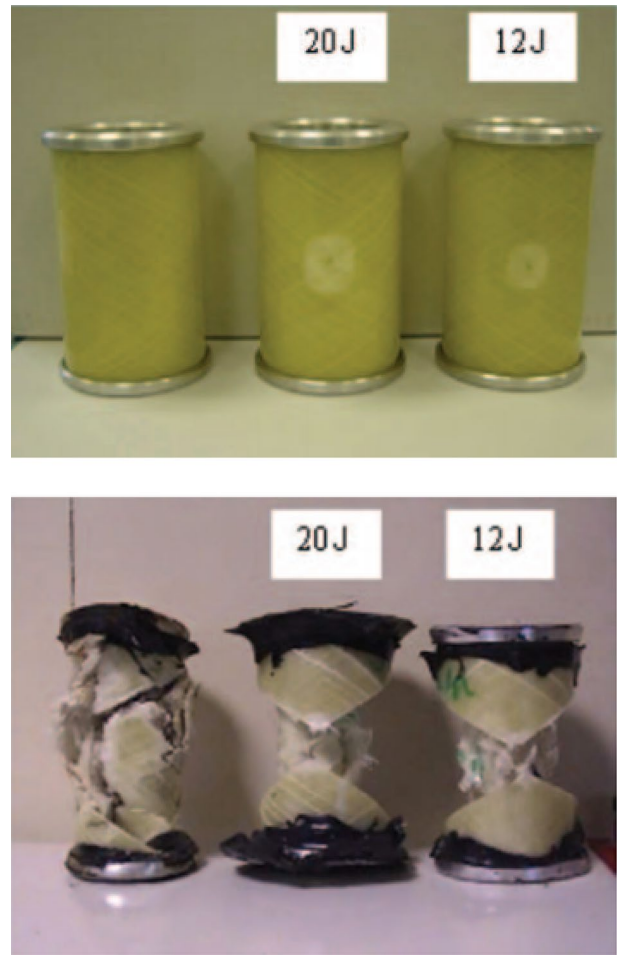

Fig. 27 Undamaged and damaged tubes before and after implosion, illustrating different failure modes in pre-damaged specimens. From [320]

Few studies have considered the effects of the shape of SHPB specimens, despite longstanding evidence of their importance. More than 45 years ago, Griffiths & Martin urged caution interpreting results for axial SHPB loading of unidirectional composite specimens [302], as "the apparent reduction in the modulus at high strain rate in this case appears to be due to the specimen geometry and not an intrinsic property of the composite." Two decades later, Harding noted there were differences between the compressive response of solid cylinders and thin waisted strip specimens [321] (Fig. 28). These differences included a larger damage area in the strip specimens at high rate which did not appear in the cylindrical specimens.

Several authors have compared specimens with different length-to-diameter (L/D) ratios. El-Habak found quite different stress–strain curves for L/D ratios of 0.85 and 1.3 [77]. Tasdemirci & Hall found the failure strains were higher in compressed woven glass/epoxy specimens with an L/D of 1 [112] compared with previous data obtained for similar

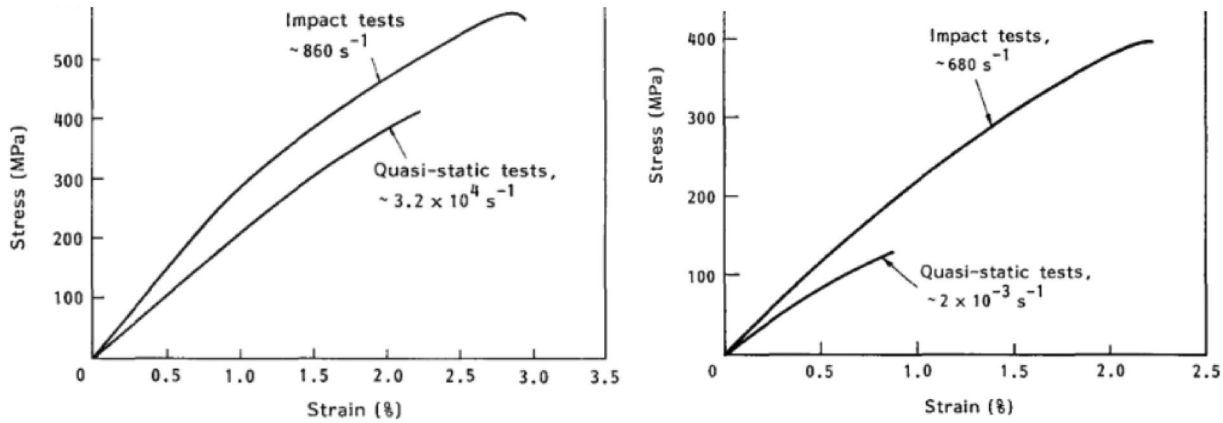

Fig. 28 Effect of strain rate on cylindrical (left) and strip (right) specimens, illustrating significant differences in overall response. From [321]

materials with an L/D of 0.5. They argued that "Since the matrix is strain rate sensitive, its yield stress increases during dynamic testing and makes it more likely that a competing deformation mechanism, such as delamination, will occur. Taller samples present (i) more locations for delamination and (ii) less interfacial constraint and, thus, produce higher strains to failure." However, two other compression studies found no statistically significant variation with shape or size [322, 323].

Pintado et al., when studying the through-thickness response, found that larger specimens were stiffer and exhibited different damage initiation characteristics [324]. Other experiments have shown that larger woven carbon/epoxy specimens are weaker under compression (perhaps due to having larger flaws), despite edge effects resulting in a discrepancy between model and experiment [325]. Ploeckl et al. [93] found that the measured compressive strength for long and thin unidirectional specimens was lower than the 'true' value derived from testing multi-directional laminates and calculating the strength of laminates only containing 0° degree fibres. Another example of unexpected rate-dependence is Heimbs et al.'s study which found that while a single-lap shear specimen with one bolt showed little or no rate dependence, an otherwise identical specimen with two bolts did show increased strength and energy absorption at $10m/s$ due to a change in failure mode from net tension to "extensive bearing and pull-through failure" [230]. Pouya et al. recently performed compression SHPB experiments on metal specimens with varying geometries as a practice run for the more complex composites [326]. However, the authors note that different geometries result in quite different wave reflections at specimen-bar interfaces, making analysis quite tricky for even this relatively straightforward experiment.

The spatial distribution of damage has been observed to depend on the rate of loading. Many authors have observed that under standard low rate tensile or compressive loads, damage localises as the stresses concentrate at weak points formed as cracks develop. By contrast, at high loading rates, damage initiation and propagation is more limited due to wave propagation effects. Therefore many smaller cracks and delaminations occur prior to failure [46, 59–61]. The interlaminar shear properties of composites (the most common failure modes) mainly depend on the properties of the polymer matrix [152], so the damage mechanisms observed are likely to be governed by the high strain rate properties of the polymer matrix which are strain rate sensitive [2].

Cantwell & Morton's 1991 review of impact resistance stated that although composites can be very strong, they are particularly weak to localised impact loading [162]. However, understanding how damage and failure occur locally is challenging. While damage during loading standard cylindrical or cuboidal specimens tends to become more widely distributed as the rate of loading is increased, the opposite may be true where the experiment results in localisation of the peak stress such as in falling wedge dropweight tests [205] and notched tensile SHPB experiments (Fig. 29) [327]. This might be because creep-like relaxation of the polymer helps relieve stress build-up between layers during impact [122], and the finite velocity of stress waves limits the rate at which energy can be dissipated from the point of impact. The anisotropic structural nature of composites again blurs the boundary between intrinsic 'material' properties and structural response. Stout et al. studied damage development in CFRPs by means of quasistatic and dynamic bend testing of beams [328]. In the quasistatic case, damage progressed gradually from multiple small matrix cracks across a large volume, followed by a small number of long delamination cracks which led to failure. In the dynamic case, damage was limited to a much smaller volume, and dominated by matrix cracking – with only a few short delamination cracks occurring (and no structural failure). This experiment again

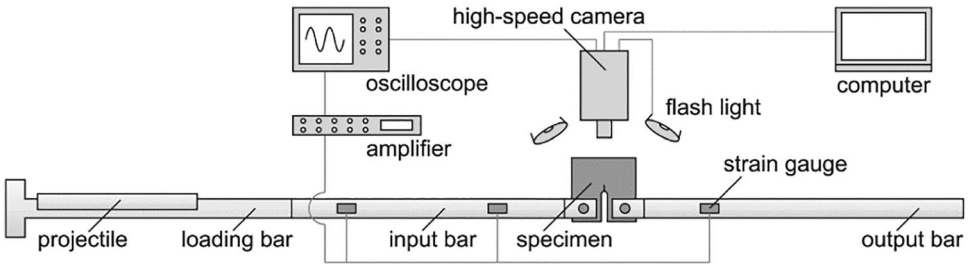

Fig. 29 SHPB setup and data acquisition for high-rate experiments studying strain-energy release rate. Where peak stress is geometrically focussed, there is evidence that under high strain rate loading the spatial distribution of damage, and accordingly failure strength/toughness is reduced. From [327]

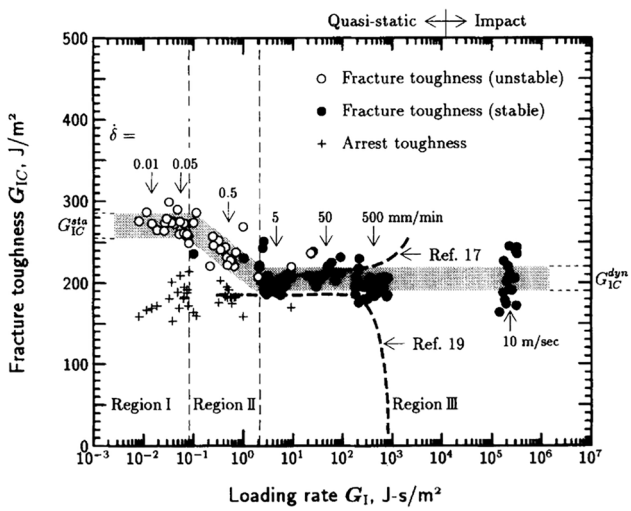

Fig. 30 Rate dependence of mode 1 interlaminar fracture toughness. From [329]

illustrates the complex relationship between damage modes, localisation and onset of failure.

When the impact or peak stress is deliberately localised, there is even more evidence of reduced toughness at high rate than for the 'simple' loading geometries discussed above. For example, in mode I wedge impact tests, Kusaka et al. (Fig. 30) observed that damage was physically limited to a smaller area at higher rates [329] as did Hoffman et al. who studied the tensile loading of notched samples [327]. Salvi et al. also reported a decrease in mode I toughness at higher loading rates in three-point bending tests [124]. Machado et al.'s experiments on falling wedge impact into double cantilever beams [330] showed there was a significant increase in toughness at higher temperatures (which they argued was due to increasing ductility of the resin) as well as a decrease in toughness with increasing rate, and Kusaka et al.'s end notched flexure tests showed a decrease in toughness with increasing shear strain rate [331] despite taking care to correct for the kinetic energy of the specimen due to dynamic fracture. Fractography of the latter showed that ductile fracture of the matrix resin, which was observed at low strain rates, was not present at high strain rates. Instead, the fracture surfaces were smooth due to debonding at the interface between reinforcing fibres and the matrix resin which required less energy per unit area to create than the ductile ones formed at low loading rates. This phenomenon was confirmed by May's review of a number of studies of the rate-dependence of mode I fracture toughness noted that for CFRPs tested at low to medium strain rates the fracture toughness decreased as the crosshead speed was increased from 4.2×10^{-6}m/s to 0.67m/s [332].

Discussion

Although there have been many studies of the high rate loading of composites, many deficiencies remain in experimental best-practice, and a consistent, unified understanding of the underlying phenomena remains elusive. Most papers have been concerned with a single material using just a few geometries and loading conditions, so quantitative comparison between materials or test conditions is lacking. The result is that there is only limited understanding of the mechanisms operating in the damage and failure of composites and their rate dependence, and so the models still most commonly employed are based on quasistatic data.

Composites should be thought of as intermediate between materials and structures rather than materials in the traditional sense that mechanical properties obtained for a small piece can be extrapolated to a product made from it. The properties of composites therefore depend not only on the intrinsic properties of the materials of which they are made, but also on the interfaces between them, their structure at all scales from micro to macro, and (what is often overlooked) the geometry and size of the specimen. Thus, for composites, techniques such as the SHPB should be considered as a form of structural analysis, which should then be combined with knowledge of the intrinsic properties of the materials that they are composed of along with their arrangement

within the structure. Indeed, the assumption made since the days of Thomas Young in the 1820s [333] that one can test a representative small element of a material and scale up the result to any size and shape of structure needs very careful consideration with respect to FRPs.

The current state of the art requires any new composite material to be tested under a range of conditions that are relevant to each particular application. However, the most useful route for future research will be carefully thought-out investigations of the underlying deformation and damage mechanisms leading to improved understanding of the relevant phenomena. The most fruitful research efforts at present appear to those that take a hybrid approach, in which in the short-term materials of interest are tested so as to reduce the risk of failure in the specific applications, but in the long-term predictive modelling capability is developed that will have wider applicability.

For tensile loading, the fibre response dominates where there are many 0° aligned fibres, strength and failure strain tend to increase, and the modulus often remains almost constant. In off-axis directions, the behaviour of the polymer matrix plays a much more important role. Since polymers tend to be much more rate-sensitive than glass and carbon fibres and usually become stiffer as the rate is increased, the off-axis properties of fibre composites also often become stiffer at increased rates. A major complication is that changes in damage failure modes can occur as the loading rate is increased. Under compressive loading, failure invariably involves lateral deformation regardless of fibre orientation, and always involves some behaviour that is controlled by the matrix. In tension and compression, where specimens of simple geometry are used, strength usually increases with strain rate, although this is not a universal finding (e.g. in-plane loading of woven materials, which may fail more readily by large-scale shear along a relatively weak interface at higher rates).

A variety of methods for loading in shear at high strain rate have been considered, and large differences in measured shear strengths have been reported by researchers who have compared several loading geometries (e.g. single vs double lap, shear vs torsion), as each method involves varying non-ideal behaviour involving stresses which are non-uniform and/or multi-dimensional. Accordingly, there is less agreement regarding the rate dependence of such behaviour. Lapped shear geometries are commonly used in the assessment of joints, for which the single lap geometry is the most straightforward option. The rate-dependence of the dynamic behaviour of such specimens is very strongly coupled with the details of the experiment, and so it is difficult if not impossible to uncover genuine trends. For bolted joints, the ratio between bolt diameter and the distance to the edges has been shown to affect the response. For bonded joints, sloping (bevelling) the edges of each lap can reduce the often considerable stress focussing at the ends of the interface section. In both bolted and bonded cases, particular care is required to ensure repeatability test to test as a slight variation in the thickness of an adhesive bond, or the tightness of fit of a bolt, can significantly affect the outcome of an experiment. Such experiments should be considered as structural tests rather than as material characterisation and are best used as a tool for model validation.

Dry ballistic experiments are a useful and efficient method of replicating geometrically complex, localised impacts in order to (i) extract some quantitative data such as energy absorption via residual velocity measurement, (ii) make qualitative comparisons (e.g. comparing failure modes), and (iii) perhaps most importantly provide a way of validating experimental models. Careful choice of orientation, layup and clamping needs to be made in order to activate or avoid certain failure modes such as delamination.

Exposure to moisture can profoundly affect the mechanical properties of composites, not only by changing the properties of the polymer matrix but also the matrix-fibre interfaces. Immersion in seawater may produce different effects to immersion in pure water, different polymers will be affected in different ways, and it can take many weeks or months for even very small specimens to become fully water-saturated. The effect on the strength of composites can be very significant and will likely depend strongly on the particular material (particularly that of the matrix) studied. 'UNDEX' blast loading and the more controlled method of ballistically-driven underwater shock offer good structural analysis tests which are useful for model validation, but complex stress states (spatially and temporally) in the water and composite make it difficult to extract quantitative 'materials' data.

Beyond the well understood rate-dependent phenomena associated with polymers employed in FRPs as matrix materials, rate-dependence manifests itself most obviously in composites through damage and failure mechanisms. For example, as the rate is increased, fibre pull-out becomes energetically unfavourable compared with fibre breakage, small cracks propagating along fibre-matrix interfaces change to cracks entirely within the matrix, and kink bands are replaced with large-scale shear failure. Often, where both stresses and materials are largely uniform, an increase in strain rate leads to initial damage being more widespread within a material. Under quasistatic loading, once a crack has opened up, that weaker location becomes a point where the stress concentrates, causing the crack to propagate. Since crack propagation takes time, many smaller cracks nucleate across a wide area under dynamic loading before any particular one reaches the point at which it results in failure. This is one mechanism lying behind the often observed increase in strength with rate.

Where a reduction in strength is observed with rate, the underlying cause usually involves a pre-existing weak point, or

region of concentrated stress, in the structure being loaded. In such a situation, applying a load more slowly can allow plastic deformation in the matrix to *reduce* the stress concentration. At higher rates there is insufficient time for this to occur, and damage is more highly localised in the already weak regions, leading to a reduction in strength with rate. Indeed, where an unexpected reduction in mechanical properties with increasing rate is observed in 'simple' specimens, it is likely that a local weakness such as a manufacturing flaw or slightly weaker interlaminar join, may be the cause.

Finally, even when strength increases with strain rate, the increased stiffness (driven primarily by polymer matrix behaviour) may result in a failure strain which is sufficiently reduced such that the toughness of the composite decreases with an increase in strain rate. This is a particular concern with respect to the durability of large composite structures, where a stiffer, more brittle response will be significantly less able to withstand a localised rapidly applied load.

New papers continue to provide data on an increasingly wide array of novel FRPs, with evolutions ranging from damage-sensing and self-repair to 3D weaves and reinforcement with carbon nanotubes. However, the ability to make best use of these innovations in high-rate applications still requires a robust understanding of the underlying physical phenomena – and accordingly the ability to develop predictive modelling capability. The complexities involved in this process for composites require us to extend beyond the traditional suite of 'materials characterisation' testing, to consider a wider range of carefully selected experimental methods (which are ultimately all to a certain extent a form of 'structural analysis', given the nature of FRPs).

The ability to draw useful equivalences between studies relies on the extent to which testing methods and the specific FRPs used are known and can be compared. As such, so performing a wider range of experiments on similar materials and methodologies (ideally using multiple specimen geometries) remains an important counterpoint to repeating the same tests on an ever-wider array of FRPs. Further, when methods such as SHPB and Plate Impact are applied to composites, we must be mindful of the extent to which 'traditional' analysis approaches can be transferred from metals and polymers to composites. For high-rate testing, the focus is often on the point of failure itself; features of the loading path, such as damage accumulation and energy absorption, often occur before dynamic equilibrium has been reached, and are thus difficult to measure – but are of particular importance when it comes to understanding FRPs.

Open Access This article is licensed under a Creative Commons Attribution 4.0 International License, which permits use, sharing, adaptation, distribution and reproduction in any medium or format, as long as you give appropriate credit to the original author(s) and the source, provide a link to the Creative Commons licence, and indicate if changes were made. The images or other third party material in this article are included in the article's Creative Commons licence, unless indicated otherwise in a credit line to the material. If material is not included in the article's Creative Commons licence and your intended use is not permitted by statutory regulation or exceeds the permitted use, you will need to obtain permission directly from the copyright holder. To view a copy of this licence, visit http://creativecommons.org/licenses/by/4.0/.

References

1. Zhang SH, Caprani CC, Heidarpour A (2018) Strain rate studies of pultruded glass fibre reinforced polymer material properties: a literature review. Constr Build Mater 171:984–1004
2. Kidane A, Gowtham Hl, Naik NK (2017) Strain rate effects in polymer matrix composites under shear loading: a critical review. J Dyn Behav Mater 3:110–132
3. Hamouda AMS, Hashmi MSJ (1998) Testing of composite materials at high rates of strain: advances and challenges. J Mater Process Technol 77:327–336
4. Dikshit V, Bhudolia SK, Joshi SC (2017) Multiscale polymer composites: a review of the interlaminar fracture toughness improvement. Fibers. https://doi.org/10.3390/fib5040038
5. Siviour CR, Walley SM (2018) Inertial and frictional effects in dynamic compression testing. In: Othman R (ed) The Kolsky-Hopkinson bar machine: selected topics. Springer, Cham, pp 205–247
6. Gama BA et al (2001) High strain-rate behavior of plain-weave S-2 glass/vinyl ester composites. J Compos Mater 35:1201–1228
7. Pan Y, Chen W, Song B (2005) Upper limit of constant strain rates in a split Hopkinson pressure bar experiment with elastic specimens. Exp Mech 45:440–446
8. Li Z, Lambros J (1999) Determination of the dynamic response of brittle composites by the use of the split Hopkinson pressure bar. Compos Sci Technol 59:1097–1107
9. Song B, Chen WN, Weerasooriya T (2003) Quasistatic and dynamic compressive behaviors of a S-2 glass/SC15 composite. J Compos Mater 37:1723–1743
10. Tuttle ME, Brinson HF (1984) Resistance-foil strain-gage technology as applied to composite materials. Exper Mech 24:54–66
11. Blitterswyk JV, Fletcher L, Pierron F (2017) Characterisation of the interlaminar properties of composites at high strain rates: a review. Adv Exp Mech 2:3–28
12. Miao C, Tippur HV (2018) Measurement of sub-micron deformations and stresses at microsecond intervals in laterally impacted composite plates using digital gradient sensing. J Dyn Behav Mater 4(3):336–358
13. Hosur MV et al (2001) High strain rate compression response of carbon/epoxy laminate composites. Compos Struct 52:405–417
14. Yokoyama T, Nakai K, Odamua T (2007) High strain rate compressive characteristics of a unidirectional carbon/epoxy composite: effect of loading directions. In: Proceedings of 2007 SEM annual conference and exposition on experimental and applied mechanics. 2007, Society for Experimental Mechanics, Bethel CT, p. 158
15. Nemat-Nasser S, Isaacs JB, Starrett JE (1991) Hopkinson techniques for dynamic recovery experiments. Proc R Soc Lond Ser A 435:371–391
16. Tzeng JT, Abrahamian AS (1995) Dynamic compressive properties of composites at interior ballistic rates of loading-experimental method. Compos Eng 5:501–508
17. Moulart R et al (2009) Full-field strain measurements at high rate on notched composites tested with a tensile Hopkinson bar.

In: Proceedings on 9th international conference on the mechanical and physical behaviour of materials under dynamic loading (DYMAT 2009). 2009, EDP Sciences, Les Ulis, France, pp 295–301
18. Moulart R et al (2011) Full-field strain measurement and identification of composites moduli at high strain rate with the virtual fields method. Exp Mech 51:509–536
19. Chen X, Li YL, Ouyang, N (2012) An SHTB-based experimental technique for elevated temperature. In: Proceedings of the 2nd international conference on electronic & mechanical engineering and information technology (EMEIT-2012). Atlantis Press, Paris. pp 321–325
20. Li G, Liu D (2014) A testing technique for characterizing composite at strain rates up to 100 s^{-1}. In: Song B, Casem D, Kimberley J (eds) Dynamic behavior of materials. Springer, Berlin, pp 73–80
21. Allazadeh MR, Wosu SN (2011) High strain rate compressive tests on woven graphite epoxy composites. Appl Compos Mater 18:311–325
22. Govender RA, Langdon GS, Nurick GN (2014) Impact bend tests using Hopkinson pressure bars. In: Song B, Casem D, Kimberley J (eds) Dynamic behavior of materials. Springer, Berlin, pp 421–426
23. Sierakowski RL (1997) Strain rate effects in composites. Appl Mech Rev 50:741–761
24. Bourne NK et al (2016) Dynamic damage in carbon-fibre composites. Philos Trans R Soc A 374:20160018
25. Frias C et al (2017) On the high-rate failure of carbon fibre composites. AIP Conf Proc 1793:110011
26. Resnyansky AD et al (2017) Impact and damage of an armour composite. AIP Conf Proc 1793:120002
27. Werner BT, Schaefer JD (2019) Calibration of a simple rate dependent elastic-plastic constitutive model for a toughened carbon epoxy composite system. Mechanics of composite, hybrid and multifunctional materials, vol 5. Springer, Cham, pp 299-301
28. Kim JH et al (2011) Effects of fiber gripping methods on single fiber tensile test using Kolsky bar. In: Proulx T (ed) Dynamic behavior of materials, vol 1: Proceedings 2010 annual conference on experimental and applied mechanics. Springer, Berlin, pp 131–136
29. Levine S, Nie Y, Chen W (2016) Dynamic transverse debonding of a single fiber. J Dyn Behav Mater 2:521–531
30. Chu JM et al (2020) Rate effects on fiber-matrix interfacial transverse debonding behavior. J Compos Mater 54:501–517
31. Favre J-P, Merienne M-C (1981) Characterization of fibre/resin bonding in composites using a pull-out test. Int J Adhesion Adhesives 1:311–316
32. Mandell JF, Chen JH, McGarry FJ (1980) A microdebonding test for in situ assessment of fibre/matrix bond strength in composite materials. Int J Adhesion Adhesives 1:40–44
33. Järvelä P et al (1983) The three-fibre method for measuring glass fibre to resin bond strength. Int J Adhesion Adhesives 3:141–147
34. Gradin PA, Bäcklund J (1981) Fatigue debonding in fibrous composites. Int J Adhesion Adhesives 1:154–158
35. Plueddemann EP (1981) Principles of interfacial coupling in fibre-reinforced plastics. Int J Adhesion Adhesives 1:305–310
36. Yi JW et al (2013) Development of high Tg epoxy resin and mechanical properties of its fiber-reinforced composites. J Appl Polym Sci 127:4328–4333
37. Michels J et al (2015) Glass transition evaluation of commercially available epoxy resins used for civil engineering applications. Compos B 77:484–493
38. Panaitescu I, Koch T, Archodoulaki VM (2019) Accelerated aging of a glass fiber/polyurethane composite for automotive applications. Polym Test 74:245–256
39. Thiruppukuzhi SV, Sun CT (2001) Models for the strain-rate dependent behavior of polymer composites. Compos Sci Technol 61:1–12
40. Mariani S (2009) Failure of layered composites subject to impacts: constitutive modeling and parameter identification issues. In: Lago GMB (ed) Strength of materials. Nova Press, Hauppage, pp 97–131
41. Karkkainen RL, Yen C-F (2012) Dynamic modeling for rate-dependent and mode-dependent cohesive interface failure analysis. J Compos Mater 46(18):2193–2201
42. Shokrieh MM, Mosalmani R, Omidi MJ (2015) A strain-rate dependent micromechanical constitutive model for glass/epoxy composites. Compos Struct 121:37–45
43. Zhang M et al (2019) The effect of temperature and strain rate on the interfacial behavior of glass fiber reinforced polypropylene composites: a molecular dynamics study. Polymers 11:11. https://doi.org/10.3390/polym11111766
44. Almahdy A, Verleysen P (2018) Challenges related to testing of composite materials at high strain rates using the split Hopkinson bar technique. EPJ Web Conf 183:02021
45. Al-Zubaidy H, Zhao X-L, Al-Mahaidi R (2013) Mechanical characterisation of the dynamic tensile properties of CFRP sheet and adhesive at medium strain rates. Compos Struct 96:153–164
46. Ou Y et al (2016) Mechanical characterization of the tensile properties of glass fiber and its reinforced polymer (GFRP) composite under varying strain rates and temperatures. Polymers 8:1. https://doi.org/10.3390/polym8050196
47. Armenàkas AE, Sciammarella CA (1973) Response of glass-fiber-reinforced epoxy specimens to high rates of tensile loading. Exper Mech 13:433–440
48. Kumar M, Naik NK (2018) Prediction of mechanical behavior of composites under high strain rate tensile loading. Mech Res Commun 90:1–7
49. Deshpande AB (2006) Characterization of CFRP and GFRP composite materials at high strain rate tensile loading. Wichita State University, Kansas, MSc Thesis
50. Asprone D et al (2009) Strain-rate sensitivity of a pultruded E-glass/polyester composite. J Compos Constr 13(6):558–564
51. Naresh K et al (2016) Effect of high strain rate on glass/carbon/hybrid fiber reinforced epoxy laminated composites. Compos B Eng 100:125–135
52. Ross CA, Cook WH, Wilson LL (1984) Dynamic tensile tests of composite materials using a split-Hopkinson pressure bar. Exper Techniques 8(11):30–33
53. Yuanming X, Xing W (1996) Constitutive equation for unidirectional composites under tensile impact. Compos Sci Technol 56(2):155–160
54. Kammerer C, Neme A (1998) Plane behaviour at high strain rates of a quasi-unidirectional E-glass/polyester composite: application to balistic impacts. Eur J Mech A Solids 17(3):461–477
55. Eskandari H, Nemes JA (2000) Dynamic testing of composite laminates with a tensile split Hopkinson bar. J Compos Mater 34(4):260–273
56. Rio TG et al (2004) Dynamic tensile behaviour at low temperature of CFRP using a split Hopkinson pressure bar. Compos Sci Technol 65(1):61–71
57. Naik NK et al (2010) High strain rate tensile behavior of woven fabric E-glass/epoxy composite. Polym Test 29(1):14–22
58. Gerlach R et al (2013) The strain rate dependent material behavior of S-GFRP extracted from GLARE. Mech Adv Mater Struct 20(7):505–514

59. Harding J, Welsh LM (1983) A tensile testing technique for fiber-reinforced composites at impact rates of strain. J Mater Sci 18(6):1810–1826
60. Ou Y, Zhu D (2015) Tensile behavior of glass fiber reinforced composite at different strain rates and temperatures. Constr Build Mater 96:648–656
61. Shokrieh MM, Omidi MJ (2009) Tension behavior of unidirectional glass/epoxy composites under different strain rates. Compos Struct 88(4):595–601
62. Welsh LM, Harding J (1985) Effect of strain rate on the tensile failure of woven reinforced polyester resin composites. Inst Phys Conf Ser 70(70):343–344
63. Lifshitz JM, Leber H (1998) Response of fiber-reinforced polymers to high strain rate loading in interlaminar tension and combined tension/shear. Compos Sci Technol 58:987–996
64. Huang Z, Nie X, Xia Y (2004) Effect of strain rate and temperature on the dynamic tensile properties of GFRP. J Mater Sci 39:3479–3482
65. Pardo S et al (2000) Tensile dynamic behaviour of unidirectional glass fibre-reinforced thermoset matrix composites. J Phys IV 10(Pr 9):359–364
66. Arao Y et al (2012) Strain-rate dependence of the tensile strength of glass fibers. J Mater Sci 47(12):4895–4903
67. Kim T, Oshima K, Kawada H (2013) Impact tensile properties and strength development mechanism of glass for reinforcement fiber. J Phys Conf Ser 451:012006
68. Taniguchi N et al (2012) Experimental study on impact tensile property of glass fiber. Adv Compos Mater 21(2):165–175
69. Barre S, Chotard T, Benzeggagh ML (1996) Comparative study of strain rate effects on mechanical properties of glass fibre-reinforced thermoset matrix composites. Compos A 27(12):1169–1181
70. Shokrieh MM, Mosalmani R, Omidi MJ (2014) Strain-rate dependent micromechanical method to investigate the strength properties of glass/epoxy composites. Compos Struct 111:232–239
71. Hallett SR, Ruiz C (1997) Material characterization tests and modelling of carbon fibre T300/914 at impact rates of strain. J Phys IV 7(C3):465–470
72. Gilat A, Goldberg RK, Roberts GD (2002) Experimental study of strain-rate-dependent behavior of carbon/epoxy composite. Compos Sci Technol 62(10–11):1469–1476
73. Taniguchi N, Nishiwaki T, Kawada H (2007) Tensile strength of unidirectional CFRP laminate under high strain rate. Adv Compos Mater 16(2):167–180
74. Taniguchi N, Nishiwaki T, Kawada H (2008) Experimental characterization of dynamic tensile strength in unidirectional carbon/epoxy composites. Adv Compos Mater 17(2):139–156
75. Okuyama I et al (2014) Dynamic and static failure behavior of notched CFRP laminate investigated by digital image correlation. Mech Time-Depend Mater 18(4):685–695
76. Kumar P, Garg A, Agarwal BD (1986) Dynamic compressive behavior of unidirectional GFRP for various fiber orientations. Mater Lett 4(2):111–116
77. El-Habak AMA (1993) Compressive resistance of unidirectional GFRP under high-rate of loading. J Compos Technol Res 15:311–317
78. Plastinin AV, Silvestrov VV (1995) Dynamic compressive strength of epoxy composites. Mech Compos Mater 31(6):549–553
79. Tay TE, Ang HG, Shim VPW (1995) An empirical strain rate-dependent constitutive relationship for glass-fibre reinforced epoxy and pure epoxy. Compos Struct 33(4):201–210
80. Oguni K, Ravichandran G (2001) Dynamic compressive behavior of unidirectional E-glass/vinylester composites. J Mater Sci 36(4):831–838
81. Ochola RO et al (2004) Mechanical behaviour of glass and carbon fibre reinforced composites at varying strain rates. Compos Struct 63(3–4):455–467
82. Pieczyska EA et al (2006) Experimental and theoretical investigations of glass-fibre reinforced composite subjected to uniaxial compression for a wide spectrum of strain rates. Arch Mech 58(3):273–291
83. Shokrieh MM, Omidi MJ (2009) Compressive response of glass–fiber reinforced polymeric composites to increasing compressive strain rates. Compos Struct 89(4):517–523
84. Acharya S et al (2017) Mechanical behaviour of glass fibre reinforced composite at varying strain rates. Mater Res Exp 4(3):035303
85. Tarfaoui M, Choukri S, Neme A (2010) Dynamic response of symmetric and asymmetric e-glass/epoxy laminates at high strain rates. Key Eng Mater 446:73–82
86. Shokrieh MM, Omidi MJ (2011) Investigating the transverse behavior of glass-epoxy composites under intermediate strain rates. Compos Struct 93(2):690–696
87. Tasdemirci A et al (2011) Experimental and Numerical Investigation of High Strain Rate Mechanical Behavior of a [0/45/90/ - 45] Quadriaxial E-Glass/Polyester Composite. Procedia Engineering 10:3068–3073
88. Naik NK et al (2010) Stress-strain behavior of composites under high strain rate compression along thickness direction: effect of loading condition. Mater Des 31(1):396–401
89. Yuan JM et al (1999) Experimental study on dynamic compressive failure of unidirectional CFRP composites. Mater Sci Res Int 5(3):202–205
90. Hsiao HM, Daniel IM (1999) Effect of fiber waviness on the high-strain-rate behavior of composites. J Thermoplast Compos Mater 12(5):412–422
91. Vaidya UK et al (2001) High strain rate response of S2-glass/epoxy composites with polycarbonate facing. Polym Polym Compos 9(2):67–80
92. Vaidya UK, Hosur MV (2003) High strain rate impact response of graphite/epoxy composites with polycarbonate facing. J Thermoplast Compos Mater 16(1):75–95
93. Ploeckl M et al (2017) A dynamic test methodology for analyzing the strain-rate effect on the longitudinal compressive behavior of fiber-reinforced composites. Compos Struct 180:429–438
94. Zhou W et al (2006) Compressive failure of carbon/epoxy laminate composites under high impact loading. Key Eng Mater 324:1237–1240
95. Powers BM et al (1997) High strain rate properties of Cycom 5920/1583 cloth glass/epoxy composites. AIAA J 35(3):553–556
96. Govender RA et al (2012) High strain rate compression testing of glass fibre reinforced polypropylene. EPJ Web Conf 26:01039
97. Arbaoui J, Tarfaoui M, Alaoui AE (2016) Mechanical behavior and damage kinetics of woven E-glass/vinylester laminate composites under high strain rate dynamic compressive loading: experimental and numerical investigation. Int J Impact Eng 87:44–54
98. Govender RA et al (2012) Determining the through-thickness properties of thick glass fiber reinforced polymers at high strain rates. J Compos Mater 46(10):1219–1228
99. Wang N, Cho C (2012) Effect of compressive loading speed and stacking sequence on mechanical characteristics of satin weave E-glass/epoxy composites. Polym Compos 33(9):1603–1612
100. Wang N, Cho C (2014) Dynamic compressive behaviors of multi directional woven composite laminates at different strain rates. Polym Polym Compos 22(2):169–175
101. Ravikumar G et al (2013) Analytical and experimental studies on mechanical behavior of composites under high strain rate compressive loading. Mater Des 44:246–255

102. Arbaoui J et al (2016) Comparative study of mechanical properties and damage kinetics of two- and three-dimensional woven composites under high-strain rate dynamic compressive loading. Int J Damage Mech 25(6):878–899
103. Arbaoui J, Tarfaoui M, El Malki Alaoui A (2016) Dynamical characterisation and damage mechanisms of E-glass/vinylester woven composites at high strain rates compression. J Compos Mater 50(24):3313–3323
104. El-Habak AMA (1991) Mechanical behaviour of woven glass fibre-reinforced composites under impact compression load. Composites 22:129–134
105. Song Z et al (2014) Mechanical behavior and failure mode of woven carbon/epoxy laminate composites under dynamic compressive loading. Compos B Eng 60:531–536
106. Li X et al (2016) Effect of strain rate on the mechanical properties of carbon/epoxy composites under quasi-static and dynamic loadings. Polym Test 52:254–264
107. Ferrero JF et al (2007) Fibre orientation effects on high strain rate of carbon/epoxy composites. Adv Compos Lett 16(1):25–31
108. Nakai K et al (2018) High strain-rate compressive properties of carbon/epoxy laminated composites: effects of loading direction and temperature. EPJ Web Conf 183:02011
109. Zou H et al (2018) The out-of-plane compression behavior of cross-Ply AS4/PEEK thermoplastic composite laminates at high strain rates. Materials 11:11. https://doi.org/10.3390/ma11112312
110. Gao GF, Li YC (2017) Dynamic behavior of a woven glass-fiber-reinforced polymer composite at high strain rates and its dynamic constitutive relationship. Mech Adv Mater Struct 24(13):1086–1093
111. Khan AS, Colak OU, Centala P (2002) Compressive failure strengths and modes of woven S2-glass reinforced polyester due to quasistatic and dynamic loading. Int J Plast 18:1337–1357
112. Tasdemirci A, Hall IW (2006) Numerical and experimental studies of damage generation in a polymer composite material at high strain rates. Polym Test 25(6):797–806
113. Hosur MV, Karim MR, Jeelani S (2004) On the response of stitched woven S2-glass/epoxy composites to high strain rate compression loading. Polym Polym Compos 12(3):183–196
114. Pagano NJ, Halpin JC (1968) Influence of end constraint in the testing of anisotropic bodies. J Compos Mater 2(1):18–31
115. Wu E, Thomas RL (1968) Off-axis test of a composite. J Compos Mater 2(4):523–526
116. Hsiao HM, Daniel IM (1998) Strain rate behavior of composite materials. Composites B 29:521–533
117. Pindera M-J, Herakovich C (1986) Shear characterization of unidirectional composites with the off-axis tension test. Exp Mech 26(1):103–112
118. Marin JC et al (2002) Determination of G12 by means of the off-axis tension test: Part I: review of gripping systems and correction factors. Compos A 33(1):87–100
119. Pierron F, Vautrin A (1997) New Ideas on the Measurement of the In-Plane Shear Strength of Unidirectional Composites. J Compos Mater 31(9):889–895
120. Sun CT, Chung I (1993) An oblique end-tab design for testing off-axis composite specimens. Composites 24(8):619–623
121. Pierron F, Vautrin A (1996) The 10 ° off-axis tensile test: A critical approach. Compos Sci Technol 56(4):483–488
122. Sayers KH, Harris B (1973) Interlaminar shear strength of a carbon fibre reinforced composite material under impact conditions. J Compos Mater 7:129–133
123. Lifshitz JM (1976) Impact strength of angle ply fiber reinforced materials. J Compos Mater 10:92–101
124. Salvi AG et al (2003) Strain rate effects on unidirectional carbon-fiber composites. AIAA J 41:2020–2028
125. Vogler TJ, Kyriakides S (1999) Inelastic behavior of an AS4/PEEK composite under combined transverse compression and shear. 1: Experiments. Int J Plast 15:783–806
126. Harizi W et al (2015) Study of the dynamic response of polymer matrix composites using an innovative hydraulic crash machine. J Dyn Behav Mater 1:359–369
127. Okoli OI, Smith GF (2000) The effect of strain rate and fibre content on the Poisson's ratio of glass/epoxy composites. Compos Struct 48:157–161
128. Ninan L, Tsai J, Sun CT (2001) Use of split Hopkinson pressure bar for testing off-axis composites. Int J Impact Eng 25(3):291–313
129. Bing Q, Sun CT (2005) Modeling and testing strain rate-dependent compressive strength of carbon/epoxy composites. Compos Sci Technol 65(15):2481–2491
130. Tsai J, Sun CT (2005) Strain rate effect on in-plane shear strength of unidirectional polymeric composites. Compos Sci Technol 65(13):1941–1947
131. Gillespie JW et al (2005) Interlaminar shear strength of plain weave S2-glass/SC79 composites subjected to out-of-plane high strain rate compressive loadings. Compos Sci Technol 65(11–12):1891–1908
132. Hsiao HM, Daniel IM, Cordes RD (1999) Strain rate effects on the transverse compressive and shear behavior of unidirectional composites. J Compos Mater 33(17):1620–1642
133. Daniel IM, Werner BT, Fenner JS (2011) Strain-rate-dependent failure criteria for composites. Compos Sci Technol 71(3):357–364
134. Daniel IM et al (2011) Characterization and constitutive modeling of composite materials under static and dynamic loading. AIAA J 49(8):1658–1664
135. Schaefer JD, Werner BT, Daniel IM (2014) Strain-rate-dependent failure of a toughened matrix composite. Exp Mech 54(6):1111–1120
136. Daniel IM (2015) Constitutive behavior and failure criteria for composites under static and dynamic loading. Meccanica 50(2):429–442
137. Vinson JR, Woldesenbet E (2001) Fiber orientation effects on high strain rate properties of graphite/epoxy composites. J Compos Mater 35(6):509–521
138. Pathan MV et al (2018) Experimental characterisation of rate-dependent compression behaviour of fibre reinforced composites. EPJ Web Conf 183:02053
139. Kuhn P, Ploeckl M, Koerber H (2015) Experimental investigation of the failure envelope of unidirectional carbon-epoxy composite under high strain rate transverse and off-axis tensile loading. EPJ Web Conf 94:01040
140. Koerber H, Xavier J, Camanho PP (2010) High strain rate characterisation of unidirectional carbon-epoxy IM7-8552 in transverse compression and in-plane shear using digital image correlation. Mech Mater 42(11):1004–1019
141. Reis VL et al (2018) Effect of fiber orientation on the compressive response of plain weave carbon fiber/epoxy composites submitted to high strain rates. Compos Struct 203:952–959
142. Weeks CA, Sun CT (1998) Modeling nonlinear rate-dependent behavior in fiber-reinforced composites. Compos Sci Technol 58:603–611
143. Shokrieh MM, Omidi MJ (2009) Investigation of strain rate effects on in-plane shear properties of glass/epoxy composites. Compos Struct 91(1):95–102
144. Gowtham HL et al (2013) High strain rate in-plane shear behavior of composites. Polym Test 32(8):1334–1341
145. Cui H et al (2016) Effect of strain rate and fibre rotation on the in-plane shear response of +/- 45 degrees laminates in tension and compression tests. Compos Sci Technol 135:106–115

146. Raju KS, Dandayudhapani S, Thorbole CK (2008) Characterization of in-plane shear properties of laminated composites at high strain rates. J Aircraft 45:493–497
147. Gilat A, Seidt JD (2018) Compression, tension and shear testing of fibrous composite with the split Hopkinson bar technique. EPJ Web Conferences 183:02006
148. Bouette B, Cazeneuve C, Oytana C (1992) Effect of strain rate on interlaminar shear properties of carbon epoxy composites. Compos Sci Technol 45(4):313–321
149. Dong L, Harding J (1994) A single-lap shear specimen for determining the effect of strain rate on the interlaminar shear strength of carbon fire-reinforced laminates. Composites 25:129–138
150. Hallett SR, Ruiz C, Harding J (1999) The effect of strain rate on the interlaminar shear strength of a carbon/epoxy cross-ply laminate: comparison between experiment and numerical prediction. Compos Sci Technol 59(5):749–758
151. Harding J, Dong L (1994) Effect of strain rate on the interlaminar shear strength of carbon-fibre-reinforced laminates. Compos Sci Technol 51:347–358
152. Gelu TA, Joshi SS, Naik NK (2011) Shear properties of acrylic under high strain rate loading. J Appl Polym Sci 121(3):1631–1639
153. Kumar P, Rai B (1988) Shear behavior of unidirectional GFRP and CFRP at high-strain rates. J Phys 49(3):97–103
154. Naik NK et al (2007) Interlaminar shear properties of polymer matrix composites: strain rate effect. Mech Mater 39(12):1043–1052
155. Laber H, Lifshitz J (1996) Interlaminar shear behavior of plain-weave GFRP at static and high rates of strain. Compos Sci Technol 56:391–405
156. Gowtham HL et al (2015) Dependency of dynamic interlaminar shear strength of composites on test technique used. Polym Test 42:151–159
157. Ruiz D et al (1990) Application of high speed photography to the study of high strain rate materials testing. Proc SPIE 1358:1134–1143
158. Nemes JA, Eskandari H, Rakitch L (1998) Effect of laminate parameters on penetration of graphite/epoxy composites. Int J Impact Eng 21(1–2):97–112
159. Yasaee M et al (2017) Strain rate dependence of mode II delamination resistance in through thickness reinforced laminated composites. Int J Impact Eng 107:1–11
160. Werner S, Dharan C (1986) The dynamic response of graphite fiber-epoxy laminates at high shear strain rates. J Compos Mater 20(4):365–374
161. Fletcher L, Van-Blitterswyk J, Pierron F (2018) Combined shear/tension testing of fibre composites at high strain rates using an image-based inertial impact test. EPJ Web Conf 183:02041
162. Cantwell WJ, Morton J (1991) The impact resistance of composite materials: a review. Composites 22(5):347–362
163. West BS (1984) Development of bird impact resistant crew enclosures for aircraft. In: Morton J (ed) Structural impact and crashworthiness, vol 2. Elsevier Applied Science, London, pp 696–709
164. Teichman HC, Tadros RN (1991) Analytical and experimental simulation of fan blade behavior and damage under bird impact. Trans ASME J Eng Gas Turbines Power 113:582–594
165. Hillsdon GK (1997) The dynamic response of scale models subjected to impact loading. Proc SPIE 2869:275–282
166. Guida M et al (2009) Design and testing of a fiber-metal-laminate bird-strike-resistant leading edge. J Aircraft 46:2121–2129
167. Shupikov AN et al (2013) Bird dummy for investigating the bird-strike resistance of aircraft components. J Aircraft 50:817–826
168. Vignjevic R et al (2013) A parametric study of bird strike on engine blades. Int J Impact Eng 60:44–57
169. Plassard F et al (2015) Experimental and numerical study of a bird strike against a windshield. EPJ Web Conf 94:01051
170. Orlando S et al (2018) Bird strike assessment for a composite wing flap. Int J Crashworthiness 23:219–235
171. Riccio A et al (2018) Numerical methodologies for simulating bird-strike on composite wings. Compos Struct 202:590–602
172. White DM, Taylor EA, Clegg RA (2003) Numerical simulation and experimental characterisation of direct hypervelocity impact on a spacecraft hybrid carbon fibre/Kevlar composite structure. Int J Impact Engng 29:779–790
173. Schonberg WP (2009) Assessing the reliability of composite structural systems and materials used in Earth-orbiting spacecraft to hypervelocity projectile impact. In: Hiermaier S (ed) Predictive modeling of dynamic processes: a tribute to Professor Klaus Thoma. Springer, Berlin, pp 397–416
174. Nam YW et al (2018) Multi-functional aramid/epoxy composite for stealth space hypervelocity impact shielding system. Compos Struct 193:113–120
175. Mackin TJ (1996) Instrumented materials testing. In: Gardner JE, Jacobs JA, Karnitz MA (eds) Standard experiments in engineering materials science and technology (NASA conference publication 3330). National Aeronautics and Space Administration, Washington DC, pp 197–216
176. Kammerer C, Neme A (1997) Plane behaviour at high strain rates of a quasi-unidirectional E-glass/polyester composite: Impact application. J Phys IV 7(C3):693–698
177. Justo J, Marquer AT (2003) High velocity impact resistance of composite materials. J Phys IV 110:651–656
178. Pattofatto S, Zhao H, Tsitsiris H (2011) Influence of the impact velocity on the perforation resistance of a glass-reinforced polypropylene material. J Reinf Plast Compos 30(13):1107–1114
179. Hou JP et al (2000) Prediction of impact damage in composite plates. Compos Sci Technol 60(2):273–281
180. Lua J et al (2004) Rate dependent multicontinuum progressive failure analysis of woven fabric composite structures under dynamic impact. Shock Vib 11(2):103–117
181. Sevkat E et al (2009) A combined experimental and numerical approach to study ballistic impact response of S2-glass fiber/toughened epoxy composite beams. Compos Sci Technol 69(7–8):965–982
182. Budhoo Y, Delale F, Liaw B (2012) Temperature effect on ballistic impact of woven graphite/epoxy composites. In: Allemang R, De Clerck J, Niezrecki C, Blough JR (eds) Topics in modal analysis II. Springer, New York, pp 413–425
183. Budhoo Y, Liaw B, Delale F (2011) Temperature effect on drop-weight impact of woven composites. In: Proulx T (ed) Dynamic behavior of materials. Springer, Berlin, pp 443–453
184. Schiffer A, Cantwell WJ, Tagarielli VL (2015) An analytical model of the dynamic response of circular composite plates to high-velocity impact. Int J Impact Eng 85:67–82
185. Miao HR et al (2019) Compos Struct 227:111343
186. Mallon S, Koohbor B, Kidane A (2015) Fracture of prestressed woven glass fiber composite exposed to shock loading. In: Song B, Casem D, Kimberley J (eds) Dynamic behavior of materials. Springer, Berlin, pp 213–219
187. Mouritz AP (2019) Advances in understanding the response of fibre-based polymer composites to shock waves and explosive blasts. Compos A 125:105502
188. Espinosa HD, Dwivedi S, Lu HC (2000) Modeling impact induced delamination of woven fiber reinforced composites with contact/cohesive laws. Comput Methods Appl Mech Eng 183(3–4):259–290
189. Tsai L et al (2009) Shock compression behavior of a S2-glass fiber reinforced polymer composite. J Appl Phys 105(9):093523

190. Mall S, Ramamurthy G (1989) Effect of bond thickness on fracture and fatigue-strength of adhesively bonded composite joints. Int J Adhesion Adhesives 9(1):33–37
191. Gorbatkina YA (2000) Correlation between the strength of fiber-reinforced plastics and the adhesive strength of fiber - matrix joints. Mech Compos Mater 36(3):169–176
192. Zachary LW, Burger CP (1980) Dynamic wave-propagation in a single lap joint. Exp Mech 20(5):162–166
193. Matthews FL, Tester TT (1985) The influence of stacking sequence on the strength of bonded CFRP single lap joints. Int J Adhesion Adhesives 5:13–18
194. Adams RD et al (1986) Stress-analysis and failure properties of carbon-fiber-reinforced-plastic steel double-lap joints. J Adhes 20(1):29–53
195. Ashcroft IA, Hughes DJ, Shaw SJ (2001) Mode I fracture of epoxy bonded composite joints. 1: Quasistatic loading. Int J Adhesion Adhesives 21:87–99
196. Farrow IR et al (2000) Impact of adhesively bonded composite joints with edge effect. Adv Compos Lett 9(6):397–408
197. Vaidya UK et al (2006) Experimental-numerical studies of transverse impact response of adhesively bonded lap joints in composite structures. Int J Adhesion Adhesives 26(3):184–198
198. Haruna K, Hamada H, Maekawa ZI (1996) Strength prediction of adhesively bonded carbon/epoxy joints. J Adhes Sci Technol 10(10):1089–1104
199. Ducept F, Davies P, Gamby D (2000) Mixed mode failure criteria for a glass/epoxy composite and an adhesively bonded composite/composite joint. Int J Adhesion Adhesives 20(3):233–244
200. Avila AF, Bueno PD (2004) Stress analysis on a wavy-lap bonded joint for composites. Int J Adhesion Adhesives 24(5):407–414
201. Khalili SMR et al (2008) Experimental study of the influence of adhesive reinforcement in lap joints for composite structures subjected to mechanical loads. Int J Adhesion Adhesives 28(8):436–444
202. Tzetzis D (2008) The role of surface morphology on the strength and failure mode of polymer fibre reinforced single lap joints. J Mater Sci 43(12):4271–4281
203. Kinloch AJ, Kodokian GA (1987) The impact resistance of structural adhesive joints. J Adhes 24(2–4):109–126
204. Blackman, B.R.K., et al., *The failure of fibre composites and adhesively bonded fibre composites under high rates of test .3. Mixed-mode I/II and mode II loadings.* Journal of Materials Science, 1996. **31**(17): p. 4467–4477.
205. Simon JC, Johnson E, Dillard DA (2005) Characterizing dynamic fracture behavior of adhesive joints under quasi-static and impact loading. J ASTM Int 2:1–19
206. Wu W et al (2013) Experimental investigation into transverse crashworthiness of CFRP adhesively bonded joints in vehicle structure. Compos Struct 106:581–589
207. Tarfaoui M, El Moumen A (2018) Dynamic behavior of top-hat bonded stiffened composite panels: experimental characterization. Compos B 149:216–226
208. Huo JS et al (2019) Experimental study on dynamic behavior of CFRP-to-steel interface. Structures 20:465–475
209. Yokoyama T (1997) Determination of impact shear strength of adhesive joints with the split Hopkinson bar. Key Eng Mater 145–149:317–322
210. Yokoyama T, Shimizu H (1998) Evaluation of impact shear strength of adhesive joints with the split Hopkinson bar. JSME Int J Ser A 41(4):503–509
211. Saleh P et al (2015) Stress homogeneity in adhesive layer of composite double lap joint under dynamic shear loading. Compos Theory Pract 15(2):101–106
212. Janin A et al (2017) An experimental technique for the characterization of adhesive joints under dynamic multiaxial loadings. Procedia Engng 197:52–59
213. Challita G et al (2009) Dynamic shear stress in a double lap bonded assembly. In: Mammoli AA, Brebbia CA (eds) Materials Characterisation. 4: Computational Methods and Experiments. WIT Press, Ashurst, UK, pp 167-173
214. Challita G, Othman R (2010) Finite-element analysis of SHPB tests on double-lap adhesive joints. Int J Adhesion Adhesives 30(4):236–244
215. Challita G et al (2011) Experimental investigation of the shear dynamic behavior of double-lap adhesively bonded joints on a wide range of strain rates. Int J Adhesion Adhesives 31(3):146–153
216. Rizk G et al (2019) Durability of composite assemblies under extreme conditions: Thermomechanical damage prediction of a double-lap bonded composite assembly subject to impact and high temperature. Compos Struct 213:58–70
217. Sassi S, Tarfaoui M, Ben Yahia H (2018) An investigation of in-plane dynamic behavior of adhesively-bonded composite joints under dynamic compression at high strain rate. Compos Struct 191:168–179
218. Sassi S, Tarfaoui M, Benyahia H (2018) Experimental study of the out-of-plane dynamic behaviour of adhesively bonded composite joints using split Hopkinson pressure bars. J Compos Mater 52(21):2875–2885
219. Tsiang TH (1984) Survey of bolted-joint technology in composite laminates. J Compos Technol Res 6:2. https://doi.org/10.1520/CTR10819J
220. Pearce GM et al (2010) Numerical investigation of dynamically loaded bolted joints in carbon fibre composite structures. Appl Compos Mater 17(3):329–346
221. Pearce GM et al (2010) Experimental investigation of dynamically loaded bolted joints in carbon fibre composite structures. Appl Compos Mater 17(3):271–291
222. Pearce GMK et al (2014) A study of dynamic pull-through failure of composite bolted joints using the stacked-shell finite element approach. Compos Struct 118:86–93
223. Sen F et al (2011) Experimental failure analysis of glass-epoxy laminated composite bolted-joints with clearance under preload. Int J Damage Mech 20(2):163–178
224. Hu J et al (2019) Modeling on bearing behavior and damage evolution of single-lap bolted composite interference-fit joints. Compos Struct 212:452–464
225. Hamada H, Haruna K, Maekawa Z (1995) Effects of stacking sequences on mechanically fastened joint strength in quasi-isotropic carbon-epoxy laminates. J Compos Tech Res 17(3):249–259
226. Içten BM, Okutan B, Karakuzu R (2003) Failure strength of woven glass fiber-epoxy composites pinned joints. J Compos Mater 37:1337–1350
227. Sarantinos N et al (2019) Micro-pins: the next step in composite-composite and metal-composite joining. Ceas Space J 11(3):351–358
228. Yang N-N et al (2019) Damage and fracture analysis of bolted joints of composite materials based on peridynamic theory. Polish Maritime Res 26(2):22–32
229. Li QM, Mines RAW, Birch RS (2001) Static and dynamic behaviour of composite riveted joints in tension. Int J Mech Sci 43(7):1591–1610
230. Heimbs S et al (2013) Static and dynamic failure behaviour of bolted joints in carbon fibre composites. Compos A Appl Sci Manuf 47:91–101
231. Perogamvros N, Lampeas G, Murphy A (2019) Experimental investigation of fastener pull-out response in composite joints

under static and dynamic loading rates. Appl Compos Mater 26(5–6):1349–1365
232. Ger GS, Kawata K, Itabashi M (1996) Dynamic tensile strength of composite laminate joints fastened mechanically. Theoret Appl Fract Mech 24(2):147–155
233. VanderKlok A, Dutta A, Tekalur SA (2013) Metal to composite bolted joint behavior evaluated at impact rates of loading. Compos Struct 106:446–452
234. Wang P et al (2015) A novel predictive model for mechanical behavior of single-lap GFRP composite bolted joint under static and dynamic loading. Compos B Eng 79:322–330
235. Rubino F et al (2020) Marine application of fiber reinforced composites: a review. J Mar Sci Eng 8:1. https://doi.org/10.3390/jmse8010026
236. Hosur MV et al (2003) Effects of temperature and moisture on the high strain rate compression response of graphite/epoxy composites. J Eng Mater Technol Trans ASME 125(4):394–401
237. Wang C et al (2004) The durability of adhesive/carbon-carbon composites joints in salt water. Int J Adhesion Adhesives 24(6):471–477
238. Filistovich DV et al (2003) Effect of moisture on the anisotropy of the dynamic shear modulus of glass-reinforced plastics. Dokl Phys 48(6):306–308
239. Woldesenbet E, Gupta N, Vinson JR (2002) Determination of moisture effects on impact properties of composite materials. J Mater Sci 37(13):2693–2698
240. Yin JY et al (2010) Modeling and simulation of corrosion mechanism for glass fiber reinforced plastic in sea water. Proc SPIE 7644:764426
241. Haque A, Hossain MK (2003) Effects of moisture and temperature on high strain rate behavior of s2-glass–vinyl ester woven composites. J Compos Mater 37(7):627–647
242. Quino G et al (2018) Measurements of the effects of pure and salt water absorption on the rate-dependent response of an epoxy matrix. Compos B Eng 146:213–221
243. Ferreira JAM et al (2002) Fatigue behaviour of composite adhesive lap joints. Compos Sci Technol 62(10–11):1373–1379
244. Mouritz AP, Saunders DS, Buckley S (1994) The damage and failure of GRP laminates by underwater explosion shock loading. Composites 25(6):431–437
245. Mouritz AP (1995) The damage to stitched GRP laminates by underwater explosion shock loading. Compos Sci Technol 55(4):365–374
246. Mouritz AP (1995) The effect of processing on the underwater explosion shock behaviour of GRP laminates. J Compos Mater 29(18):2488–2503
247. Mouritz AP (1995) The effect of underwater explosion shock loading on the fatigue behavior of GRP laminates. Composites 26(1):3–9
248. Mouritz AP (1996) The effect of underwater explosion shock loading on the flexural properties of grp laminates. Int J Impact Eng 18(2):129–139
249. LeBlanc J, Shukla A (2010) Dynamic response and damage evolution in composite materials subjected to underwater explosive loading: An experimental and computational study. Compos Struct 92(10):2421–2430
250. LeBlanc J, Shukla A (2011) Dynamic response of curved composite panels to underwater explosive loading: experimental and computational comparisons. Compos Struct 93(11):3072–3081
251. Gauch E, LeBlanc J, Shukla A (2012) Response of preloaded thin composite panels subjected to underwater explosive loading. Comput Struct 112:342–353
252. LeBlanc J, Shukla A (2015) Underwater explosion response of curved composite plates. Compos Struct 134:716–725
253. Motley MR, Young YL, Liu Z (2011) Three-dimensional underwater shock response of composite marine structures. J Appl Mech 78(6):061013
254. Dulnev AI, Nekliudova EA (2017) Resistance of GPS samples to non-contact underwater explosion. J Phys Conf Ser 919:012003
255. Rolfe E et al (2017) Failure analysis using X-ray computed tomography of composite sandwich panels subjected to full-scale blast loading. Compos B 129:26–40
256. Gauch E, LeBlanc J, Shukla A (2018) Near field underwater explosion response of polyurea coated composite cylinders. Compos Struct 202:836–852
257. Ren LJ et al (2019) Blast response of water-backed metallic sandwich panels subject to underwater explosion - experimental and numerical investigations. Compos Struct 209:79–92
258. McCoy RW, Sun CT (1997) Fluid-structure interaction analysis of a thick-section composite cylinder subjected to underwater blast loading. Compos Struct 37(1):45–55
259. O'Daniel J et al (2000) Numerical simulations and precision impact testing for the development of an UNDEX response validation methodology. In: Brebbia CA (ed) Structures under shock and impact VI. WIT Press, Southampton, pp 299–308
260. Gong SW, Lam KY (1998) Transient response of stiffened composite submersible hull subjected to underwater explosive shock. Compos Struct 41(1):27–37
261. Gong SW, Lam KY (1999) Transient response of floating composite ship section subjected to underwater shock. Compos Struct 46(1):65–71
262. Gong SW, Lam KY (2002) Analysis of layered composite beam to underwater shock including structural damping and stiffness effects. Shock Vib 9(6):283–291
263. Deshpande VS, Fleck NA (2005) One-dimensional response of sandwich plates to underwater shock loading. J Mech Phys Solids 53(11):2347–2383
264. Fatt MSH, Palla L (2009) Analytical modeling of composite sandwich panels under blast loads. J Sandwich Struct Mater 11(4):357–380
265. Fathallah E et al (2015) Numerical investigation of the dynamic response of optimized composite elliptical submersible pressure hull subjected to non-contact underwater explosion. Compos Struct 121:121–133
266. Gong SW, Khoo BC (2015) Transient response of stiffened composite submersible hull to underwater explosion bubble. Compos Struct 122:229–238
267. Gao Y, Oterkus S (2018) Peridynamic analysis of marine composites under shock loads by considering thermomechanical coupling effects. J Mar Sci Eng. https://doi.org/10.3390/jmse6020038
268. Espinosa HD, Lee S, Moldovan N (2006) A novel fluid structure interaction experiment to investigate deformation of structural elements subjected to impulsive loading. Exp Mech 46(6):805–824
269. Latourte F et al (2011) Failure mechanisms in composite panels subjected to underwater impulsive loads. J Mech Phys Solids 59:1623–1646
270. Wei XD et al (2013) Three-dimensional numerical modeling of composite panels subjected to underwater blast. J Mech Phys Solids 61(6):1319–1336
271. Avachat S, Zhou M (2012) Effect of facesheet thickness on dynamic response of composite sandwich plates to underwater impulsive loading. Exp Mech 52(1):83–93
272. Avachat S, Zhou M (2017) Novel experimental and 3D multiphysics computational framework for analyzing deformation and failure of composite laminates subjected to water blasts. Int J Impact Eng 106:223–237
273. Avachat S, Zhou M (2014) Response of cylindrical composite structures to underwater impulsive loading. Proc Eng 88:69–76

274. Avachat S, Zhou M (2015) High-speed digital imaging and computational modeling of dynamic failure in composite structures subjected to underwater impulsive loads. Int J Impact Eng 77:147–165
275. Qu T, Avachat S, Zhou M (2017) Response of cylindrical composite structures subjected to underwater impulsive loading: experimentations and computations. Trans ASME: J Eng Mater Technol 139:021020
276. Avachat S, Zhou M (2016) High-speed digital imaging and computational modeling of hybrid metal-composite plates subjected to water-based impulsive loading. Exp Mech 56(4):545–567
277. Schiffer A, Tagarielli VL (2012) The response of rigid plates to blast in deep water: fluid & structure interaction experiments. Proc R Soc A 468(2145):2807–2828
278. Schiffer A et al (2012) The response of composite plates to underwater blast. Int Mech Eng Congr Expos 8(2012):749–758
279. Schiffer A, Tagarielli VL (2014) The one-dimensional response of a water-filled double hull to underwater blast: experiments and simulations. Int J Impact Eng 63:177–187
280. Schiffer A, Tagarielli VL (2014) One-dimensional response of sandwich plates to underwater blast: fluid-structure interaction experiments and simulations. Int J Impact Eng 71:34–49
281. Schiffer A, Tagarielli VL (2015) The response of circular composite plates to underwater blast: experiments and modelling. J Fluids Struct 52:130–144
282. Huang W et al (2018) Dynamic response of circular composite laminates subjected to underwater impulsive loading. Compos A 109:63–74
283. Ren P et al (2018) Experimental investigation on dynamic failure of carbon/epoxy laminates under underwater impulsive loading. Mar Struct 59:285–300
284. Zhang P, Porfiri M (2019) A combined digital image correlation/particle image velocimetry study of water-backed impact. Compos Struct 224:111010
285. Owens, A.C., et al. *Underwater Impact of Composite Structures*. in *Proceedings of the ASME Pressure Vessels and Piping Conference 2010, Vol 4*. 2010. American Society of Mechanical Engineers. p. 231–240
286. Kwon YW (2011) Study of fluid effects on dynamics of composite structures. J Pressure Vessel Technol 133(3):031301
287. Wu X-F et al (2008) Experimental characterization of the impact damage tolerance of a crossply graphite fiber/epoxy laminate. Polym Compos 29:534–543
288. Mouritz AP, Leong KH, Herszberg I (1997) A review of the effect of stitching on the in-plane mechanical properties of fibre-reinforced polymer composites. Compos A Appl Sci Manuf 28(12):979–991
289. Kendall K (1981) Dislocations at adhesive interfaces in composites. Int J Adhesion Adhesives 1:301–304
290. Minnaar K (2004) A novel technique for time-resolved detection and tracking of interfacial and matrix fracture in layered materials. J Mech Phys Solids 52(12):2771–2799
291. Lee D et al (2009) Experimental study of dynamic crack growth in unidirectional graphite/epoxy composites using digital image correlation method and high-speed photography. J Compos Mater 43(19):2081–2108
292. Bi X et al (2002) Dynamic fiber debonding and frictional push-out in model composite systems: numerical simulations. Mech Mater 34(7):433–446
293. Li ZH et al (2002) Dynamic fiber debonding and frictional push-out in model composite systems: experimental observations. Exp Mech 42(4):417–425
294. Tamrakar S, Haque BZ, Gillespie JW (2016) High rate test method for fiber-matrix interface characterization. Polym Testing 52:174–183
295. Mahmood H, Dorigato A, Pegoretti A (2019) Temperature dependent strain/damage monitoring of glass/epoxy composites with graphene as a piezoresistive interphase. Fibers 7:2. https://doi.org/10.3390/fib7020017
296. Woo S, Kim T (2018) Peak frequency analysis via wavelet transform for impact damage mechanisms in woven composites. J Mech Sci Technol 32(6):2601–2612
297. Riccio A et al (2014) Delamination buckling and growth phenomena in stiffened composite panels under compression. Part I: An experimental study. J Compos Mater 48(23):2843–2855
298. Duchene P et al (2018) A review of non-destructive techniques used for mechanical damage assessment in polymer composites. J Mater Sci 53(11):7915–7938
299. Saeedifar M et al (2019) Using passive and active acoustic methods for impact damage assessment of composite structures. Compos Struct 226:111252
300. Xue YD et al (2019) Acoustic emission and X-ray computed microtomography characterization of damage accumulation in a woven C-f/SiC composite. Mater Charact 155:109748
301. Russo S (2013) Damage assessment of GFRP pultruded structural elements. Compos Struct 96:661–669
302. Griffiths LJ, Martin DJ (1974) A study of the dynamic behaviour of a carbon-fibre composite using the split Hopkinson pressure bar. J Phys D: Appl Phys 7:2329–2341
303. Taniguchi N, Nishiwaki T, Kawada H (2005) Evaluating the mechanical properties of a CFRP tube under a lateral impact load using the split Hopkinson bar. Adv Compos Mater 14(3):263–276
304. Minak G et al (2010) Low-velocity impact on carbon/epoxy tubes subjected to torque - experimental results, analytical models and FEM analysis. Compos Struct 92(3):623–632
305. Tsai JL, Chen KH (2007) Characterizing nonlinear rate-dependent behaviors of graphite/epoxy composites using a micromechanical approach. J Compos Mater 41(10):1253–1273
306. Allix O, Feissel P, Thévenet P (2003) A delay damage mesomodel of laminates under dynamic loading: basic aspects and identification issues. Comput Struct 81(12):1177–1191
307. Gupta JS et al (2005) Fracture prediction of a 3D C/C material under impact. Compos Sci Technol 65(3):375–386
308. Petrov, Y. *Incubation time based fracture mechanics*. in *Proc. of the 19th European Conference on Fracture. Fracture Mechanics for Durability, Reliability and Safety. Kazan, Russia*. 2012.
309. Lataillade JL et al (1996) Effects of the intralaminar shear loading rate on the damage of multiply composites. Int J Impact Eng 18(6):679–699
310. Li ZY, Ghosh S (2020) Micromechanics modeling and validation of thermal-mechanical damage in DER353 epoxy/borosilicate glass composite subject to high strain rate deformation. Int J Impact Eng 136:103414
311. Tarfaoui M, El Moumen A, Ben Yahia H (2018) Damage detection versus heat dissipation in E-glass/epoxy laminated composites under dynamic compression at high strain rate. Composite Struct 186:50–61
312. Adachi T et al (2000) Evaluation of dynamic fracture toughness of unidirectional CFRP laminates. JSME Int J Ser A 43(2):179–185
313. Kuhn P et al (2017) Fracture toughness and crack resistance curves for fiber compressive failure mode in polymer composites under high rate loading. Compos Struct 182:164–175
314. Leite LFM et al (2018) Strain rate effects on the intralaminar fracture toughness of composite laminates subjected to tensile load. Compos Struct 201:455–467
315. Daryadel SS et al (2015) Energy absorption of pultruded hybrid glass-graphite epoxy composites under high strain-rate SHPB compression loading. Mater Sci Applic 6:511–518

316. Tarfaoui M, Nachtane M, El Moumen A (2019) Energy dissipation of stitched and unstitched woven composite materials during dynamic compression test. Compos B 167:487–496
317. Li LJ et al (2019) Repeated low-velocity impact response and damage mechanism of glass fiber aluminium laminates. Aerosp Sci Technol 84:995–1010
318. Oleg AS et al (2019) Experimental study of the influence of preliminary complex mechanical loads on the deformation and strength properties of polymer composites. Proc Struct Integr 18:757–764
319. Aktas A (2005) Bearing strength of carbon epoxy laminates under static and dynamic loading. Compos Struct 67(4):485–489
320. Tarfaoui M, Gning PB, Collombet F (2007) Residual strength of damaged glass/epoxy tubular structures. J Compos Mater 41(18):2165–2182
321. Harding J (1993) Effect of strain-rate and specimen geometry on the compressive strength of woven glass-reinforced epoxy laminates. Composites 24(4):323–332
322. Centala PK, Qian ZF, Khan AS (1997) Experimental and analytical investigation on the compressive response of GRP plain woven thick composite. Proc SPIE 2921:446–451
323. Woldesenbet E, Vinson JR (1999) Specimen geometry effects on high-strain-rate testing of graphite/epoxy composites. AIAA J 37(9):1102–1106
324. Pintado P et al (2001) Experimental investigation of the dynamic response of graphite-epoxy composite laminates under compression. Compos Struct 53(4):493–497
325. Liu T, Sun B, Gu B (2017) Influence of specimen size and inner defects on high strain rates compressive behaviors of plain woven composites. Polym Test 64:55–64
326. Pouya M et al (2018) Dynamic behavior of geometrically complex hybrid composite samples in a Split-Hopkinson Pressure Bar system. IOP Conf. Ser. Mater. Sci. Eng 373:012025
327. Hoffmann J, Cui H, Petrinic N (2018) Determination of the strain-energy release rate of a composite laminate under high-rate tensile deformation in fibre direction. Compos Sci Technol 164:110–119
328. Stout MG et al (1999) Damage development in carbon/epoxy laminates under quasi-static and dynamic loading. Compos Sci Technol 59(16):2339–2350
329. Kusaka T et al (1998) Rate dependence of mode I fracture behaviour in carbon-fibre/epoxy composite laminates. Compos Sci Technol 58(3–4):591–602
330. Machado JJM et al (2019) Dynamic behaviour in mode I fracture toughness of CFRP as a function of temperature. Theoret Appl Fract Mech 103:102257
331. Kusaka T, Yamauchi Y, Kurokawa T (1994) Effects of strain-rate on mode-ii interlaminar fracture-toughness in carbon-fiber epoxy laminated composites. J Phys IV 4(C8):671–676
332. May M (2016) Measuring the rate-dependent mode I fracture toughness of composites–A review. Compos A Appl Sci Manuf 81:1–12
333. Young T (1826) On the cohesive strength of different metals. J Franklin Inst 2:120–123

Publisher's Note Springer Nature remains neutral with regard to jurisdictional claims in published maps and institutional affiliations.